

Imperial College London  
Department of Mathematics

# **Majorana dynamics of spinor Bose-Einstein condensates**

Azmat Habibullah

Submitted in part fulfilment of the requirements  
for the degree of MSci Mathematics at  
Imperial College London, June 2021



I hereby declare that this thesis and the work reported herein was composed by and originated entirely from me. Information derived from the published and unpublished work of others has been acknowledged in the text and references are given in the list of sources.

Azmat Habibullah (2020)

The copyright of this thesis rests with the author and is made available under a Creative Commons Attribution Non-Commercial No Derivatives licence. Researchers are free to copy, distribute or transmit the thesis on the condition that they attribute it, that they do not use it for commercial purposes and that they do not alter, transform or build upon it. For any reuse or redistribution, researchers must make clear to others the licence terms of this work.

---

## Abstract

In this paper we derive equations governing the dynamics of the Majorana stellar representation (MSR) of spinor Bose-Einstein condensates (BEC). We do this under the single-mode approximation in zero potential in the absence of Zeeman effects. We first provide an overview of the MSR: a description of a spin- $F$  state as  $2F$  spin-1/2 states, each represented as a point (star) on the unit sphere. Using geometric techniques, we derive expressions for the Berry phase and connection of spin-1 states in terms its representative stars, building on existing results. Then, we show that for spin-1 condensates, the motion of the aforementioned system is two vectors precessing with a fixed angle about their barycenter, which is a constant of the motion. Using the expressions derived earlier, we compute the Berry phase for this regime. Finally, we present a method for estimating an s-wave scattering coefficient based on the time period of the oscillation of the Majorana dynamics, before touching briefly on aspects of the spin-2 dynamics.

---

## Acknowledgements

I would firstly like to thank Ryan Barnett, my supervisor, for his continued guidance and support throughout the year. I would also like to thank Lucas Spencer for many intriguing conversations, as well as providing suggestions for this report, and Hugo Chu for providing assistance with numerical computations.

I extend my sincerest thanks to Sulaimaan Lim, whose insights helped keep me focused and Aaron-Naidoo Bagwell for proof-reading parts of this report.

It is my privilege to thank Shivan Parmar, whose curious perspective on life and admirable pursuit of mathematics has kept me spirited throughout school and university.

I owe a deep sense of gratitude to Saleem Raza, whose enthusiasm for materials science initially piqued my curiosity in condensed matter physics, and whose thirst for knowledge has continually inspired me throughout my degree.

---

Throughout this paper, a range of commonly-known formulae are used. They are listed here for convenience.

**Trigonometric**

$$\cos \frac{x}{2} = \pm \sqrt{\frac{1 + \cos x}{2}} \quad (1)$$

$$\sin \frac{x}{2} = \pm \sqrt{\frac{1 - \cos x}{2}} \quad (2)$$

$$\cos^2 x = \frac{1 + \cos 2x}{2} \quad (3)$$

$$\sin^2 x = \frac{1 - \cos 2x}{2} \quad (4)$$

$$\tan(\pi/2 - x) = \cot x \quad (5)$$

$$\tan \theta/2 - \cot \theta/2 = \cot \theta \quad (6)$$

**Vector Calculus**

$$(\vec{a} \times \vec{b}) \cdot (\vec{c} \times \vec{d}) = (\vec{a} \cdot \vec{c})(\vec{b} \cdot \vec{d}) - (\vec{a} \cdot \vec{d})(\vec{b} \cdot \vec{c}) \quad (7)$$

# Contents

<b>Abstract</b>	<b>3</b>
<b>Acknowledgements</b>	<b>4</b>
<b>1 Introduction</b>	<b>8</b>
References . . . . .	12
<b>2 Background</b>	<b>14</b>
2.1 Spin-1/2 . . . . .	14
2.1.1 Geometry of the Bloch sphere . . . . .	16
2.2 Majorana's stellar representation . . . . .	16
2.2.1 Mathematical formulation . . . . .	17
2.2.2 Examples and useful results . . . . .	18
2.3 Berry phase, connection and curvature . . . . .	21
References . . . . .	24
<b>3 Geometrical interpretations of Berry phase</b>	<b>27</b>
3.1 Berry curvature . . . . .	27
3.2 Berry phase . . . . .	28
3.2.1 Spin 1 . . . . .	32
References . . . . .	35
<b>4 Bose-Einstein condensates</b>	<b>36</b>
4.1 Introduction . . . . .	37
4.2 Spin 1 . . . . .	38
4.2.1 Dynamics . . . . .	39
4.2.2 Berry phase . . . . .	43
4.3 Spin 2 . . . . .	44
References . . . . .	46
<b>5 Conclusion</b>	<b>49</b>
References . . . . .	51
<b>A Numerics</b>	<b>52</b>
References . . . . .	52

# List of Figures

1.1	xkcd 1861 . . . . .	11
2.1	Visualisations of example states on Bloch sphere . . . . .	15
2.2	Example Majorana representations: the spin 1.5 state (left) has 3 repeated points at the North pole and the spin 3 state (right) has points forming a regular hexagon	19
2.3	Examples of Corollories 2.2.3.1 and 2.2.3.2 . . . . .	21
4.1	Time evolution of eigenstates of $\vec{m} \cdot \vec{S}$ under $c_0 = 0$ . . . . .	42
4.2	Time evolution of states with given initial conditions under $c_0 = 0$ . Purple is the start of the trajectory, yellow is the end. . . . .	43
4.3	Time evolution of states with given initial conditions. Purple is the start of the trajectory, yellow is the end. On the left, the state is symmetric about the $x$ axis and the dynamics are confined to the region $y < 0$ . On the right, the dynamics are trivially stationary. . . . .	46
5.1	xkcd 793 . . . . .	50

# Chapter 1

## Introduction

*“Nobody really understands quantum mechanics.”*

---

Richard Feynman

Over the last century, quantum mechanics has become a frontier of modern physics, describing how light and matter behave with unerring accuracy. Modern-day technology, including lasers, transistors and magnetic resonance imaging in healthcare, relies extensively on quantum phenomena. The fascinating yet bizarre nature of the quantum realm continues to inspire generations of students (see Figure 1.1), motivated by the theoretical and experimental breakthroughs in the field. This paper brings together three key developments in modern quantum mechanics: spin, Bose-Einstein condensates and Berry’s phase.

‘Spin’ as a concept was first proposed by Wolfgang Pauli in 1925 [1] as an intrinsic form of angular momentum, or an internal degree of freedom, but its experimental origin dates back to 1922, in the Stern-Gerlach experiment. In this experiment, a beam of silver atoms was fired through a magnetic field onto a photographic plate [2, 3, 4]. Classically, it was expected that the beam would have a continuous spread, showing a continuous line on the plate, but instead, the beam split into 2 distinct points. Stern and Gerlach intended to demonstrate the quantisation of angular momentum according to Bohr’s so-called ‘old’ quantum theory (now referred to as old as it is accepted to be incorrect). The results matched Bohr’s prediction, but it was realised shortly afterwards that the interpretation of the Stern-Gerlach experiment

was incorrect. The experiment had in fact measured the internal spin degree of freedom of the electron - unbeknownst to the duo at the time as the concept did not yet exist! It was not until 1927 that theoreticians realised that Stern and Gerlach's work had measured the electron's spin. Soon after, Markus Fierz proved the spin statistics theorem in 1939 [5] showing that particles could be classified as either: *fermions*, which have half-integer spin, or *bosons*, which have integer spin. His argument was generalised by Pauli in 1940 [6], who in the same paper also extended his result from 1925 that identical fermions can not occupy the same quantum state, now known as the Pauli exclusion principle.

Pauli's exclusion principle highlights one of the key differences between fermions and bosons and has huge ramifications: bosons have no restriction regarding occupying the same quantum state. As the theory of spin was being developed, in 1924, Jagdish Chandra Bose developed some ideas on the statistics of photons [7] and Albert Einstein built on these in 1925 [8], predicting that a sufficiently large number of bosons could occupy the same quantum state at a sufficiently low temperature. A system in this regime is called a *Bose-Einstein condensate* (BEC). It was shown that these systems would have extremely interesting properties, for example being linked to the superfluidity of helium [9]. However, the temperatures required to achieve Bose-Einstein condensation are so close to absolute zero that for a long time it was virtually impossible to observe them. Consequently, relatively little was done until 1995, when the first BEC was experimentally realised using rubidium atoms in a single spin state [10]. Not long after, in 1998, influential papers by Tin Lun Ho [11] and Tetsuo Ohmi and Kazushige Machida [12] paved the way for significantly more work in this area, which remains an active area of research today.

Spin plays an important role in the theory of BECs. Since BECs require extremely low temperatures, they are incredibly unstable. Most experimental realisations require them to be 'trapped'. This is mostly done via magnetic and optical traps. In the case of magnetic traps, the spin degrees of freedom of the condensate are frozen. This does not occur in the cases of optical traps. We distinguish between these two cases by referring to the former case as *scalar* BECs and the latter case as *spinor* BECs. More broadly, different spins result in characteristically different behaviours. In this paper we will focus on (spin-1 and 2) spinor BECs.

Mathematically, spin-1/2 states can be described by a 2-dimensional complex vector. A

priori, such a quantity has 4 (real) degrees of freedom, but with some work these states can be visualised on a 3-dimensional sphere, the Bloch sphere. This suffices for spin-1/2 systems, but the exact construction cannot be repeated for higher spins. In a relatively understated work, Ettore Majorana outlined a new geometric idea enabling visualisation of arbitrary spin systems on the unit sphere [13]. In particular, his method provided a means of visualizing a spin- $F$  state as  $2F$  states (also referred to as points or stars) on the unit sphere. This is called Majorana's stellar representation (MSR).

We require one more important ingredient. In 1984, Michael Berry, generalising results from the 1950s, found that under certain conditions, a quantum system evolving adiabatically ('slowly' in a sense) remains in its initial state, up to a phase [14]. This phase has two contributions - one contribution is related to the time evolution of the state, and the other on the set of parameters the system depends on. The former is the *dynamical phase* and the latter is the *Berry phase*. The Berry phase reveals the underlying geometric nature of quantum mechanics and has applications in many areas of physics, including magnetism, Hall effects and the classification of insulators [15].

This paper brings together all of the aforementioned ideas. In particular, we analyse the dynamics of spinor BECs in the context of the MSR and Berry phase.

Chapter 2 covers background material on which we build throughout the paper. Section 2.1 provides a summary of visualising spin-1/2 states via the Bloch sphere. Having done this for spin-1/2 systems, section 2.2 outlines how to extend this to visualise a spin- $F$  state as  $2F$  spin-1/2 states, and thus  $2F$  points on the Bloch sphere, using the MSR. Finally, Section 2.3 is a recap of adiabatic quantum mechanics and Berry's phase. This chapter is mostly background material apart from a few key results used later.

Chapter 3 focuses on geometrical approaches to linking the Berry phase with the MSR. In this chapter we derive existing results from a few papers in more detail and extend these for use in Chapter 4. Section 3.1 provides an interpretation of the Berry curvature for spin-1/2 systems in terms of an area element. Section 3.2 extends this discussion to spin-1 systems, eventually deriving results for the Berry phase in terms of the MSR.

Chapter 4 applies the theory we have developed to spinor BECs. Section 4.1 provides

background on the development of BECs. We then analyse BEC equations of motion for spin 1 and 2 sections in Sections 4.2 and 4.3 respectively. The spin 1 dynamics have a natural interpretation in the MSR whereas the spin 2 dynamics are significantly more complicated. Finally, using the theory developed in chapter 3, we relate the Berry phase for these states to the Berry phase for states in the MSR. In particular, we conclude that the Berry phase for eigenstates of the spin 1 system is just the sum of the Berry phase for states in the Majorana representation. Additionally, the Majorana dynamics provide us with a way of estimating scattering lengths. Apart from the background information, this chapter is entirely original.

Chapter 5 summarises results from this paper and discusses avenues for further research.

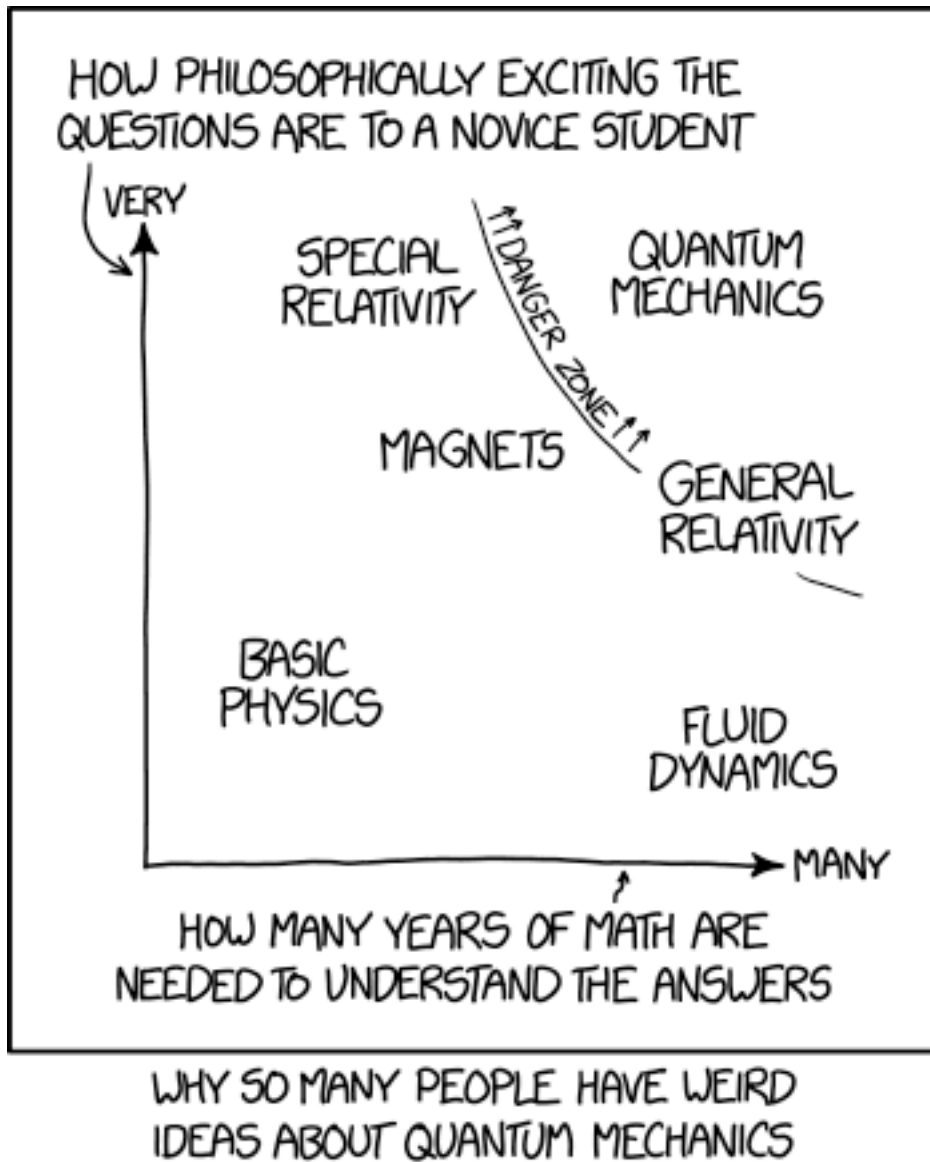


Figure 1.1: xked 1861

## References

- [1] W. Pauli, “Über den Zusammenhang des Abschlusses der Elektronengruppen im Atom mit der Komplexstruktur der Spektren,” *Zeitschrift für Physik*, vol. 31, no. 1, pp. 765–783, 1925.
- [2] W. Gerlach and O. Stern, “Der experimentelle Nachweis der Richtungsquantelung im Magnetfeld,” *Zeitschrift für Physik*, vol. 9, no. 1, pp. 349–352, 1922.
- [3] W. Gerlach and O. Stern, “Der experimentelle Nachweis des magnetischen Moments des Silberatoms,” *Zeitschrift für Physik*, vol. 8, no. 1, pp. 110–111, 1922.
- [4] W. Gerlach and O. Stern, “Das magnetische Moment des Silberatoms,” *Zeitschrift für Physik*, vol. 9, no. 1, pp. 353–355, 1922.
- [5] M. Fierz, “Über die relativistische Theorie kräftefreier Teilchen mit beliebigem Spin,” *Helvetica Physica Acta*, vol. 12, pp. 3–37, Jan. 1939.
- [6] W. Pauli, “The Connection Between Spin and Statistics,” *Physical Review*, vol. 58, pp. 716–722, Oct. 1940.
- [7] Bose, “Plancks Gesetz und Lichtquantenhypothese,” *Zeitschrift für Physik*, vol. 26, no. 1, pp. 178–181, 1924.
- [8] A. Einstein, “Quantum Theory of a Monoatomic Ideal Gas A translation of Quantentheorie des einatomigen idealen Gases ( Einstein , 1924 ),” *Sitzungsberichte der Preuss. Akad. der Wissenschaften*, vol. 1, no. 3, 1925.
- [9] F. London, “On the Bose-Einstein Condensation,” *Physical Review*, vol. 54, pp. 947–954, Dec. 1938.
- [10] M. H. Anderson, J. R. Ensher, M. R. Matthews, C. E. Wieman, and E. A. Cornell, “Observation of Bose-Einstein Condensation in a Dilute Atomic Vapor,” *Science*, vol. 269, pp. 198 LP – 201, July 1995.

- [11] T. L. Ho, “Spinor bose condensates in optical traps,” *Physical Review Letters*, vol. 81, no. 4, pp. 742–745, 1998.
- [12] T. Ohmi and K. Machida, “Bose-Einstein condensation with internal degrees of freedom in alkali atom gases,” *Journal of the Physical Society of Japan*, vol. 67, pp. 1822–1825, Nov. 1998.
- [13] E. Majorana, “Atomi orientati in campo magnetico variabile,” *Il Nuovo Cimento*, vol. 9, no. 2, 1932.
- [14] M. Berry, “Quantal phase factors accompanying adiabatic changes,” *Proceedings of the Royal Society of London. A. Mathematical and Physical Sciences*, vol. 392, pp. 45–57, Mar. 1984.
- [15] B. A. Bernevig, *Topological Insulators and Topological Superconductors*. Princeton University Press, stu - stud ed., 2013.

# Chapter 2

## Background

*“Einstein said that if quantum mechanics were correct then the world would be crazy. Einstein was right - the world is crazy.”*

---

Daniel M. Greenberger

We begin with a review of the Bloch sphere. We then see how to naturally extend this visualisation to systems with higher spin and close the chapter with a review of the Berry phase.

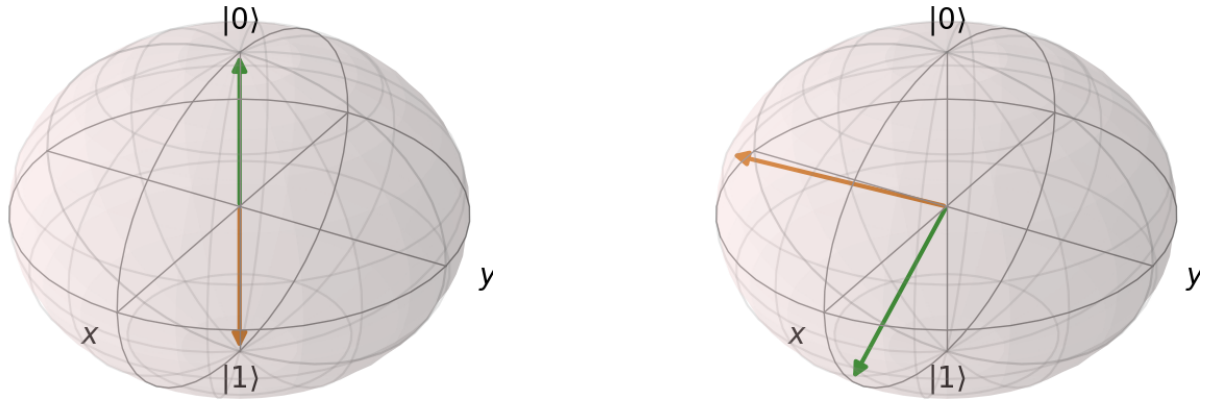
### 2.1 Spin-1/2

For a spin-1/2 particle with orthonormal basis  $|\uparrow\rangle = |1/2, 1/2\rangle, |\downarrow\rangle = |1/2, -1/2\rangle$ , we may write a state as  $|\psi\rangle = a|\uparrow\rangle + b|\downarrow\rangle$  for  $a, b \in \mathbb{C}$ . As the Hilbert space in quantum mechanics is projective, only the relative phase between  $a$  and  $b$  has physical meaning, so we can fix the phase of  $a$ . By convention, we choose  $a$  to be real and positive. We further require normalisation:  $\langle\psi|\psi\rangle = |a|^2 + |b|^2 = 1$ . These two constraints reduce the degrees of freedom to 2. We can thus parametrise  $a$  and  $b$  by writing

$$|\psi\rangle = \cos \theta/2 |\uparrow\rangle + e^{i\phi} \sin \theta/2 |\downarrow\rangle \text{ or for convenience } \psi = (\cos \theta/2, e^{i\phi} \sin \theta/2)^1 \quad (2.1)$$

---

<sup>1</sup>We will use this streamlined notation throughout the paper



(a) Basis spinors  $\psi_{green} = (1, 0)$ ,  $\psi_{orange} = (0, 1)$

(b)  $\psi_{green} = (1, 2)$ ,  $\psi_{orange} = (3 + 5i, 4)$  (normalised)

Figure 2.1: Visualisations of example states on Bloch sphere

for  $0 \leq \theta \leq \pi$ ,  $0 \leq \phi < 2\pi$ . This representation is always unique as the point represented by  $\theta$  and  $\phi$  is unique. We identify this spinor with spherical polar coordinates  $(\theta, \phi)$  on the unit sphere  $r = 1$  (the physics ISO convention) with Cartesian representation  $\vec{m} = (\sin \theta \cos \phi, \sin \theta \sin \phi, \cos \theta)$ . However,  $\vec{m}$  can also be recognised as the expectation value of the spin operators in the state  $\psi^2$ : with  $\vec{\sigma} = (\hat{\sigma}_x, \hat{\sigma}_y, \hat{\sigma}_z)$  the Pauli vector, the vector of spin-1/2 matrices, we have that  $\vec{m} = \langle \hat{\sigma} \rangle$ . Noting that quantum mechanical observables are necessarily expectations, the Bloch sphere thus shows the direction a state is ‘pointing’ in, or ‘most spinning’ in.

Figure 2.1 shows examples of states visualised on the Bloch sphere, and consequently which direction the spins for these states ‘most point in’. Note that the states  $|\uparrow\rangle$  and  $|\downarrow\rangle$  correspond to the north and south pole respectively. These states are orthogonal in Hilbert space, but do not correspond to the orthogonal basis vectors in  $\mathbb{R}^3$ . This is due to the factor of 2 in the parametrisation in equation 2.1 - the physical interpretation is states cannot be both spin up and down at the same time, but can have a non-zero measurement in e.g. both the  $x$  and  $z$  directions at the same time.

In summary, the Bloch sphere provides a useful way of visualising a spin-1/2 quantum state.

<sup>2</sup>This is why we choose a parametrisation for equation 2.1 in terms of  $\frac{\theta}{2}$  when in fact  $k\theta$  suffices for any  $k \in \mathbb{R}$ : the factor of 2 is required to have the physical interpretation of the Bloch sphere representation ‘pointing in the direction of the spin’. This is a manifestation of the double cover of  $SU(2)$  onto  $SO(3)$ .

It is by no means the only way of geometrically interpreting states - see for example [1], where states are visualised instead on unit disks - but it is very commonly used and we shall use it extensively in this paper. It is heavily used to study density matrices [2]; quantum computation [3]; optics [4] (where it is often called the Poincaré sphere) and more [5, 6].

### 2.1.1 Geometry of the Bloch sphere

As a side remark, it is important to note that the Bloch sphere is not a sphere in the most basic sense. Consider the poles:  $\theta = 0$  corresponds to  $|\uparrow\rangle$ , but  $\theta = \pi$  corresponds to  $e^{i\phi}|\downarrow\rangle$  for  $\phi \in [0, 2\pi)$  - the south pole is multivalued. This degenerate point cannot be removed and highlights the fact that the Bloch sphere is topologically a sphere, but geometrically a hemisphere (the south pole corresponds to the equator). Interested readers can study the geometry of Hopf fibrations [7, 8] but this is beyond the scope of this text.

## 2.2 Majorana's stellar representation

Given the useful geometric insight provided by the Bloch sphere, one can ask whether higher spin states can be represented in a similar way.

Let us first consider a spin-1 spinor  $\psi = (a, b, c) \in \mathbb{C}^3$ , with 6 real degrees of freedom. As in the spin-1/2 case we can remove 2 degrees of freedom via normalisation and a global phase, leaving 4 degrees of freedom. This cannot be represented on the 2-sphere as we would like, so we require another approach.

Notice that the spin-1 (spinor) has twice the degrees of freedom of the spin-1/2 (spinor). We can therefore try to represent the spin-1 as two spin-1/2s and visualise each of these on the Bloch sphere, providing a geometrical interpretation of the original spin-1/2 state. It turns out that this is possible: more generally, we can represent a spin- $F$  as  $2F$  symmetrised spin-1/2 points on the Bloch sphere (symmetrised in the sense that order does not matter). This idea was initially presented as a side remark by Ettore Majorana<sup>3</sup> in 1932 [10] - to him, this was so

---

<sup>3</sup>Although discovered in the context of quantum mechanics, Majorana's discovery applies more generally to visualise the complex projective space  $\mathbb{C}\mathbf{P}^n$  - it follows that  $\mathbb{C}\mathbf{P}^n = \mathbf{S}^2 \times \mathbf{S}^2 \times \dots \times \mathbf{S}^2 / S_n$ , where  $S_n$  is the symmetric group of permutations of  $n$  objects [9]

obvious that it required just 4 lines of development! The 17-year-old Julian Schwinger stumbled upon this paper in 1935 and was perplexed - he spent a considerable amount of time on his own calculations before matching Majorana's results in 1937 [11], although he left, in his own words, "the most important part of the paper [showing he matched Majorana's result] implicit" [12]. Despite this representation providing a revolutionary way of interpreting angular momentum in quantum mechanics, the works by Majorana and Schwinger remain relatively unknown<sup>4</sup>. We now provide some motivation for Majorana's interpretation.

The idea is as follows: associate a polynomial to each point in  $\mathbb{C}^n$  and the roots of this polynomial to points in  $\mathbb{CP}^{n-1}$ , then identify the roots with the stars<sup>5</sup>. In order to make such a visualisation with  $2F$  points (or stars) useful, we demand some key properties. Since the representation is reducing to the Bloch sphere, we demand that  $SU(2)$  transformations correspond to ordinary rotations of the sphere. To do this, we demand a state of spin 'up' in the direction given by the unit vector  $\vec{m}$  to be represented by  $n = 2F$  points sitting at the point where  $\vec{m}$  meets the sphere. This generalises naturally: demand a state that is an eigenstate of  $\vec{m} \cdot \vec{F}$  with eigenvalue  $k$  to be represented by  $F + k$  points at this point and  $F - k$  points at the antipode. Note that since we are working with roots of a polynomial, the Majorana representation leaves out information about the phase [16].

### 2.2.1 Mathematical formulation

More precisely, consider a spin- $F$  state  $\psi = \sum_{\alpha=-F}^F A_\alpha |\alpha\rangle = (A_F, \dots, A_F)$ , where  $F_z |\alpha\rangle = \alpha |\alpha\rangle$  and the  $A_\alpha$  are a set of normalised complex coefficients. The polynomial we identify with the spinor  $\psi$ , which we shall refer to as the *characteristic polynomial*, is

$$f_\psi(\zeta) = \sum_{\alpha=0}^{2F} \sqrt{\binom{2F}{\alpha}} A_{F-\alpha}^* \zeta^\alpha$$

The  $2F$  complex roots of  $f_\psi(\zeta)$  are identified uniquely with spherical polars via stereographic

---

<sup>4</sup>The historical development is fascinating. Discussions can be found in Schwinger's own words [12] and expositions on the subject [13, 14]

<sup>5</sup>Theoretically, since a spin  $F$  irreducible representation of  $SU(2)$  has dimension  $2F + 1$  and all irreducible representations of  $SU(2)$  are symmetric tensor products of the fundamental spinor representation, every finite dimensional Hilbert space can be thought of as a symmetric tensor product of fundamental  $SU(2)$  representation spaces [15]

projection  $\zeta_k = \tan \frac{\theta_k}{2} e^{i\phi_k}$ , and thus uniquely determine the coefficients  $A_\alpha$  and therefore  $|\psi\rangle$  up to normalisation and an overall phase factor (a motivation for this can be found in [9]).

Recall that the time reversal operator  $\hat{T}$  satisfies the anti-commutation relation  $\{\hat{T}, i\} = 0$  and its action on a general spin- $F$  spinor is  $(\hat{T}\psi)_m = (-1)^m \psi_{F-m}^*$ . This corresponds to taking the roots  $z_i \mapsto \frac{-1}{z_i^*}$ , which just corresponds to the antipodal point on the sphere<sup>6</sup>.

### 2.2.2 Examples and useful results

This section provides some examples to help understand the stellar representation and consists of some original calculations which will be used in later sections, as well as some examples to help visualise the stellar representation. Corollaries 2.2.3.1 and 2.2.3.2 in particular will be relied upon later. We also touch on applications of the stellar representation in other fields.

Firstly, note that the spin-1/2 stellar representation reduces to the standard Bloch sphere representation:

$$|\zeta_{1/2}\rangle = \sum_{\alpha=0}^1 \sqrt{\binom{1}{\alpha}} \zeta^\alpha |F - \alpha\rangle = \zeta^0 |1\rangle + \zeta |0\rangle = |1\rangle + e^{i\phi} \tan \theta/2 |0\rangle$$

and the magnitude of this state is  $1 + \tan^2 \theta/2 = \sec^2 \theta/2$ , so the normalised spinor is  $\psi_{1/2} = (\cos \theta/2, e^{i\phi} \sin \theta/2)$ , as expected.

The following results and figures provide specific examples of states.

**Theorem 2.2.1.** *The spin- $F$  state  $|m\rangle$  corresponds to  $m + F |\uparrow\rangle$  states.*

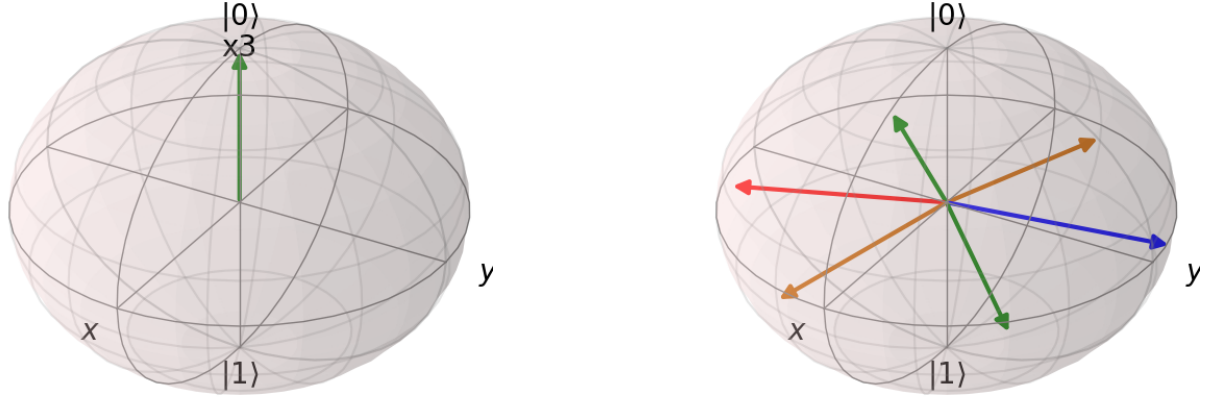
*Proof.* This is by construction - in full detail, represent the state  $|\psi\rangle = |m\rangle$  as the spinor  $e_{m+F}$ , where  $e_i$  is the canonical  $i$ th basis vector. The characteristic polynomial is

$$f_\psi(\zeta) = \sum_{\alpha=0}^{2F} \sqrt{\binom{2F}{\alpha}} A_{F-\alpha}^* \zeta^\alpha = \sum_{\alpha=0}^{2F} \sqrt{\binom{2F}{\alpha}} \delta_{F+m-\alpha} \zeta^\alpha = \sqrt{\binom{2F}{F+m}} \zeta^{F+m}$$

which has  $F + m$  repeated 0s as roots. For each complex root  $\zeta = 0$  we have  $\theta = 0 \pmod{2\pi}$  and  $\phi = 0 \pmod{2\pi}$ , which corresponds to the state  $|\uparrow\rangle$  on the Bloch sphere.  $\square$

---

<sup>6</sup>The defining polynomial for the Majorana representation is often taken as (what we have described as) the time-reversed one, that is,  $f_\psi(\zeta) = \sum_{\alpha=0}^{2F} (-1)^\alpha \sqrt{\binom{2F}{\alpha}} A_\alpha \zeta^{2F-\alpha}$  [9]


 (a) Spin 1.5  $\psi = (1, 0, 0, 0)$ 

 (b) Spin 3  $\psi = (3, 0, 0, 0, 0, 0, 5i)$ 

Figure 2.2: Example Majorana representations: the spin 1.5 state (left) has 3 repeated points at the North pole and the spin 3 state (right) has points forming a regular hexagon

**Theorem 2.2.2.** *The spin- $F$  state  $|\psi\rangle = a|m\rangle + b|-m\rangle$  corresponds to a polygon of degree  $m$  on the sphere.*

*Proof.* Let  $|\psi\rangle = a|m\rangle + b|-m\rangle$ . The characteristic polynomial is

$$\begin{aligned}
 0 = f_\psi(\zeta) &= \sum_{\alpha=0}^{2F} \sqrt{\binom{2F}{\alpha}} A_{F-\alpha}^* \zeta^\alpha \\
 &= \sqrt{\binom{2F}{0}} a^* \zeta^0 + \sqrt{\binom{2F}{2F}} b^* \zeta^{2F} \\
 &= a^* \zeta^{2F} + b^* = 0 \\
 \implies \zeta^{2F} + \left(\frac{a}{b}\right)^* &= 0
 \end{aligned}$$

These are the  $2F$ -th roots of unity, with complex roots  $z, z\omega, \dots, z\omega^{2F-1}$  where  $z = \sqrt[2F]{-\left(\frac{a}{b}\right)^*} = \sqrt[2F]{re^{i\nu}} = \sqrt[2F]{r}e^{i\nu/2F}$  and  $\omega = e^{i\pi/F}$ . Then  $\theta = 2 \arctan(|z|)$  and the  $\phi_k = \frac{\nu}{2F} + \frac{k\pi}{F}$  for  $k = 0, \dots, 2F - 1$ . Thus permuting  $1 \rightarrow i$  etc corresponds to rotating  $\frac{\pi}{4m}$   $\square$

In the literature a specific example of the above states are referred to as NOON states [9]: this is because, in the angular momentum eigenbasis/Dicke basis  $|j+m, j-m\rangle = |n-k, k\rangle'$  the NOON states corresponding to equidistant stars around the equator are

$$|NOON\rangle = |n, 0\rangle' + |0, n\rangle' = |n/2, n/2\rangle + |n/2, -n/2\rangle$$

where we have rewritten in our basis for comparison with Theorem 2.2.2 (with  $a = 1, b = -1$ ).

The NOON states have applications to quantum metrology [9] and quantum optics [14].<sup>7</sup>

**Theorem 2.2.3.** *The spinor corresponding to points  $(\theta_1, \phi_1), (\theta_2, \phi_2)$  is*

$$\psi = \begin{pmatrix} e^{-i(\phi_1+\phi_2)} \tan \frac{\theta_1}{2} \tan \frac{\theta_2}{2} \\ -(e^{-i\phi_1} \tan \frac{\theta_1}{2} + e^{-i\phi_2} \tan \frac{\theta_2}{2})/\sqrt{2} \\ 1 \end{pmatrix}$$

*Proof.* The roots of the characteristic polynomial are  $e^{i\phi_1} \tan \frac{\theta_1}{2}, e^{i\phi_2} \tan \frac{\theta_2}{2}$ . The polynomial is thus

$$\left(\zeta - e^{i\phi_1} \tan \frac{\theta_1}{2}\right) \left(\zeta - e^{i\phi_2} \tan \frac{\theta_2}{2}\right) = \zeta^2 - \zeta \left(e^{i\phi_1} \tan \frac{\theta_1}{2} + e^{i\phi_2} \tan \frac{\theta_2}{2}\right) + e^{i(\phi_1+\phi_2)} \tan \frac{\theta_1}{2} \tan \frac{\theta_2}{2}$$

By definition  $f_\psi(\zeta) = \sum_{\alpha=0}^2 \sqrt{\binom{2}{\alpha}} A_{1-\alpha}^* \zeta^\alpha$  so we read off  $A_{1-\alpha}^*$  and therefore  $A$  as stated.  $\square$

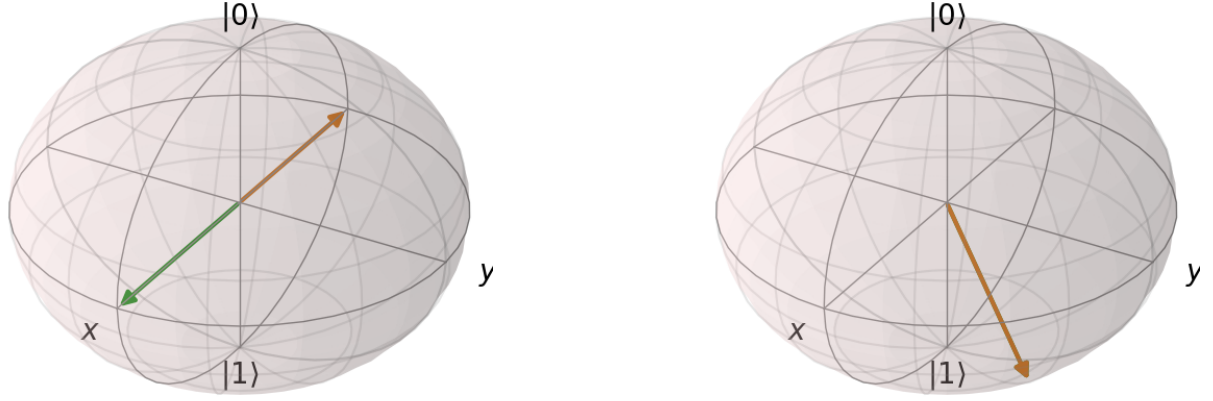
**Corollary 2.2.3.1.** *The spinor for antipodal points given  $(\theta, \phi)$  is*

$$\psi = \begin{pmatrix} -e^{-2i\phi} \\ -e^{-i\phi} \cot \theta / \sqrt{2} \\ 1 \end{pmatrix}$$

*Proof.*  $\vec{n}_1 = -\vec{n}_2$  graphically corresponds to antipodal points. In spherical coordinates the point antipodal to  $(\theta, \phi)$  is  $(\pi - \theta, \phi + \pi)$ . By Theorem 2.2.3 and trigonometric identities 5 and 6,

---

<sup>7</sup>As an interesting aside, the state  $\psi = (1, 1, \dots, 1)$  yields the polynomial  $\sum_{\alpha=0}^{2F} \sqrt{\binom{2F}{\alpha}} \zeta^\alpha$ . This seemingly simple polynomial is not well-studied, but we can say a bit about its roots. It is a palindromic real polynomial, so its roots either lie on the unit circle (when the conjugate is also the reciprocal of the root) or there are sets of 4 roots of form  $\alpha, \bar{\alpha}, 1/\alpha, 1/\bar{\alpha}$  that do not lie on the unit circle [17]. For  $F < 10$ , the roots all lie on the unit circle, but we see a divergence for higher  $F$ .


 (a) Antipodal points at  $(\theta, \phi) = (\pi/2, \pi)$ 

 (b) Repeated points at  $(\theta, \phi) = (\pi/3, \pi/4)$ 

Figure 2.3: Examples of Corollaries 2.2.3.1 and 2.2.3.2

$$\psi = \begin{pmatrix} e^{-i(2\phi+\pi)} \tan \frac{\theta}{2} \tan \frac{\pi-\theta}{2} \\ -(e^{-i\phi} \tan \frac{\theta}{2} + e^{-i(\phi+\pi)} \tan \frac{\pi-\theta}{2})/\sqrt{2} \\ 1 \end{pmatrix} = \begin{pmatrix} -e^{-2i\phi} \tan \frac{\theta}{2} \cot \frac{\theta}{2} \\ -e^{-i\phi} (\tan \frac{\theta}{2} - \cot \frac{\theta}{2})/\sqrt{2} \\ 1 \end{pmatrix} = \begin{pmatrix} -e^{-2i\phi} \\ -e^{-i\phi} \cot \theta/\sqrt{2} \\ 1 \end{pmatrix}$$

□

**Corollary 2.2.3.2.** *The spinor for repeated points at  $(\theta, \phi)$  is*

$$\psi = \begin{pmatrix} e^{-2i\phi} \tan^2 \frac{\theta}{2} \\ -\sqrt{2} e^{-i\phi} \tan \frac{\theta}{2} \\ 1 \end{pmatrix}$$

*Proof.* This follows immediately from Theorem 2.2.3 with  $\theta = \theta_1 = \theta_2, \phi = \phi_1 = \phi_2$ . □

## 2.3 Berry phase, connection and curvature

In a seminal paper in 1984, Michael Berry showed that a system undergoing adiabatic evolution in an eigenstate of a Hamiltonian remains in the same eigenstate but obtains a phase factor [18]. This phase has a contribution from the state's time evolution, which is called its *dynamical*

*phase*, and a contribution from variation of the eigenstate with the changing Hamiltonian, which is called its *Berry* or *geometric phase*. The Berry phase has associated with it the Berry connection and the Berry curvature tensor, which we define below. The curvature is gauge invariant, whereas the connection and phase are not; the phase is gauge invariant modulo  $2\pi$ .

These quantities are more pervasive than they may initially seem - in particular, they are of importance outside of the adiabatic regime too. For example, the Berry phase explains the Aharonov-Bohm effect, in which a charged particle is affected by an electromagnetic potential despite being confined to a region of zero electromagnetic field<sup>8</sup> [18, 19]. Further, the Berry phase and curvature have a related topological invariant called the Chern number, which is critical in quantum hall physics<sup>9</sup> and the field of topological insulators<sup>10</sup> [21].

In this paper we will focus mostly on the Berry phase and its relationship with the Majorana representation. The remainder of this section outlines some key properties of the Berry phase. We begin with the Quantum Adiabatic Theorem and the relevant definitions.

**Theorem 2.3.1** (Quantum Adiabatic Theorem). *For a slowly varying Hamiltonian  $\hat{H} = \hat{H}(\vec{R})$  depending continuously on a set of real parameters  $\vec{R}(t)$  in the time range  $T$ , the solution of the Schrodinger equation  $\Psi(t)$  with initial conditions  $\Psi(0) = \psi_n(0)$ , where  $\psi_n(t)$  is the  $n$ th instantaneous eigenstate satisfying  $\hat{H}(\vec{R}) |\psi_n, \vec{R}\rangle = E_n(\vec{R}) |\psi_n, \vec{R}\rangle$ , may be approximated as*

$$\|\Psi(t) - \psi_{adiabatic}(t)\| \approx o\left(\frac{1}{T}\right)$$

where the adiabatic approximation is

$$|\psi_{adiabatic}(t)\rangle = e^{i\theta_n(t)} e^{i\gamma_n(t)} |\psi_n(t)\rangle$$

Here,  $\theta_n(t) = -\frac{1}{\hbar} \int_0^t E_n(t') dt'$  is the *dynamical phase* and  $\gamma_n(t) = \oint_C a_n \cdot d\vec{R}$  is the *Berry phase*, with  $a_n = i \langle \psi_n | \nabla_{\vec{R}} | \psi_n \rangle$  the *Berry connection*, where  $C$  is a closed curve in parameter space such that  $|\psi_n, \vec{R}\rangle$  is single-valued and differentiable along  $C$ . The *Berry curvature* for the

---

<sup>8</sup>This discovery developed the idea that the vector potential is genuinely ‘physical’ - it was previously thought of as only a mathematical convenience.

<sup>9</sup>For example, the Hall conductivity can be written terms of the Chern number, which is quantised [20]

<sup>10</sup>Here, the Berry phase plays a role similar to that of genus in the Gauss-Bonnet theorem from geometry.

$n$ -th eigenstate is  $f_{n,\alpha\beta} = \frac{\partial}{\partial R^\alpha} a_{n,\beta} - \frac{\partial}{\partial R^\beta} a_{n,\alpha}$  (the  $n$  is frequently dropped for convenience).

**Lemma 2.3.2.** *The Berry phase is real.*

*Proof.* Note that  $\langle \psi_n | \psi_n \rangle = 1$  so

$$0 = \nabla \langle \psi_n | \psi_n \rangle = \langle \nabla \psi_n | \psi_n \rangle + \langle \psi_n | \nabla \psi_n \rangle = a_n + a_n^* = 2\text{Re}(a_n)$$

Consequently, the Berry connection and thus Berry phase are real.  $\square$

**Lemma 2.3.3** (Gauge freedom of Berry phase). *The Berry phase is gauge invariant modulo  $2\pi$*

*Proof.* For any given eigenstate  $|\psi\rangle$  of  $\hat{H}$ , we have that  $|\psi'\rangle = e^{-i\alpha} |\psi\rangle$  is an equally valid eigenstate of  $\hat{H}$ . Further, provided  $\alpha(T) = \alpha(0) + 2\pi n$  for  $n \in \mathbb{Z}$  we have that  $|\psi'(T)\rangle = |\psi'(0)\rangle$ .

Now

$$\begin{aligned} \gamma' &= i \int_0^t \langle \psi' | \dot{\psi}' \rangle dt' = i \int_0^t \langle \psi' | -i\dot{\alpha} e^{-i\alpha} \psi + e^{-i\alpha} \dot{\psi} \rangle dt' \\ &= -i^2 \int_0^t \dot{\alpha} e^{i\alpha} e^{-i\alpha} \langle \psi | \psi \rangle dt' + i \int_0^t e^{i\alpha} e^{-i\alpha} \langle \psi | \dot{\psi} \rangle dt' \\ &= \gamma + 2\pi n \end{aligned}$$

$\square$

The typical example of Berry phase is that of a spin in a magnetic field. Suppose a spin-half particle is under the effect of a slowly varying magnetic field of constant magnitude  $\hat{H} = -\vec{B}(t) \cdot \vec{\sigma}$  with  $\vec{B}(0) = \vec{B}(T)$ .

In three dimensions, we may express the eigenstates as

$$\begin{aligned} |\uparrow_n\rangle &= \cos \frac{\theta}{2} |\uparrow\rangle + e^{i\phi} \sin \frac{\theta}{2} |\downarrow\rangle \\ |\downarrow_n\rangle &= \sin \frac{\theta}{2} |\uparrow\rangle - e^{i\phi} \cos \frac{\theta}{2} |\downarrow\rangle \end{aligned}$$

where  $|\uparrow\rangle, |\downarrow\rangle$  are eigenstates of  $\sigma_z$ .

We first compute the Berry connection:

$$\begin{aligned}
 a_\phi^\uparrow &= i \langle \uparrow_n | \nabla_\phi | \uparrow_n \rangle \\
 &= i \left( \cos \frac{\theta}{2} \langle \uparrow | + e^{-i\phi} \sin \frac{\theta}{2} \langle \downarrow | \right) \left( i e^{i\phi/2} \sin \frac{\theta}{2} | \downarrow \rangle \right) \\
 &= -\sin^2 \frac{\theta}{2}
 \end{aligned}$$

Similarly,  $a_\phi^\downarrow = -\cos^2 \frac{\theta}{2}$ ,  $a_\theta^\uparrow = a_\theta^\downarrow = 0$ . Consequently for the  $|\downarrow\rangle$  state the Berry curvature is  $f_{\theta\phi} = \partial_\theta a_\phi - \partial_\phi a_\theta = \frac{1}{2} \sin \theta$ . Upon a change of phase, for example taking the  $|\downarrow\rangle$  eigenstate to be  $e^{-i\phi} \sin \frac{\theta}{2} |\uparrow\rangle - e^{i\phi} \cos \frac{\theta}{2} |\downarrow\rangle$ , the connection changes to  $a_\phi^\downarrow = \sin^2 \frac{\theta}{2}$  but the curvature is unchanged<sup>11</sup>. The Berry phase for a given curve can be computed using the connection - for the curve given by  $\theta = \pi/2$ ,  $\phi \in [0, 2\pi)$  we have  $\gamma = -1/2 \int_0^{2\pi} d\phi = -\pi$ . This is  $-1/2$  times the solid angle subtended by the path, an example of a more general result which we prove in the next chapter.

## References

- [1] M. Ozols, “Geometry of a qubit,” *Pre-Print*, vol. 1, no. Id 20286921, pp. 1–17, 2007.
- [2] O. Gamel, “Entangled Bloch spheres: Bloch matrix and two-qubit state space,” *Physical Review A*, vol. 93, p. 062320, June 2016.
- [3] R. Laflamme, E. Knill, C. Negrevergne, R. Martinez, S. Sinha, and D. G. Cory, “Introduction to NMR quantum information processing,” *Proceedings of the International School of Physics “Enrico Fermi”*, vol. 148, pp. 411–439, 2002.
- [4] M. Cherchi, F. Sun, M. Kapulainen, M. T. Harjanne, and T. Aalto, “Flat-top interleavers based on single MMIs,” p. 14, SPIE-Intl Soc Optical Eng, Feb. 2020.
- [5] A. Kent and D. Pitalúa-García, “Bloch-sphere colorings and Bell inequalities,” *Physical Review A - Atomic, Molecular, and Optical Physics*, vol. 90, p. 062124, Dec. 2014.

---

<sup>11</sup>Note also that the integral of the Berry curvature over the whole sphere is  $2\pi$ . The factor of  $2\pi$  is not a coincidence - the quantity we have calculated is the Chern number, which is quantised in units of  $2\pi$

- [6] S. Tamate, K. Ogawa, and M. Kitano, “Bloch-sphere representation of three-vertex geometric phases,” *Physical Review A - Atomic, Molecular, and Optical Physics*, vol. 84, Nov. 2011.
- [7] M. Mosseri, R.; Monastyrsky, “Two-Qubit and Three-Qubit Geometry and Hopf Fibrations,” in *Topology in Condensed Matter*, ch. 9, pp. 187–203, Springer, Berlin, Heidelberg, 2006.
- [8] R. Mosseri and R. Dandoloff, “Geometry of entangled states, Bloch spheres and Hopf fibrations,” *Journal of Physics A: Mathematical and General*, vol. 34, pp. 10243–10252, Nov. 2001.
- [9] P. Society and J. Univer, *Geometry of Quantum States: An Introduction to Quantum Entanglement*. 2004.
- [10] E. Majorana, “Atomi orientati in campo magnetico variabile,” *Il Nuovo Cimento*, vol. 9, no. 2, 1932.
- [11] J. Schwinger, “On nonadiabatic processes in inhomogeneous fields,” *Physical Review*, vol. 51, pp. 648–651, Apr. 1937.
- [12] J. Schwinger, “The Majorana formula,” *Transactions of the New York Academy of Sciences*, vol. 38 II, pp. 170–184, Nov. 1977.
- [13] M. S. Rogalski and S. B. Palmer, “Comments concerning Julian Schwinger’s “ON ANGULAR MOMENTUM”,” 2002.
- [14] S. Shabbir, *Majorana Representation in Quantum Optics Doctoral Thesis in Physics*. No. 2, 2017.
- [15] N. Jeevanjee, “Basic Representation Theory BT - An Introduction to Tensors and Group Theory for Physicists,” pp. 145–212, Boston: Birkhäuser Boston, 2011.
- [16] Y. Kawaguchia and M. Uedaa, “Spinor Bose-Einstein condensates,” *Physics Reports*, vol. 520, no. 5, pp. 253–381, 2012.

- [17] J. Konvalina and V. Matache, “Palindrome-Polynomials with Roots on the Unit Circle,” *Comptes Rendus Mathématiques*, vol. 26, Jan. 2004.
- [18] M. Berry, “Quantal phase factors accompanying adiabatic changes,” *Proceedings of the Royal Society of London. A. Mathematical and Physical Sciences*, vol. 392, pp. 45–57, Mar. 1984.
- [19] Y. Aharonov and D. Bohm, “Significance of electromagnetic potentials in the quantum theory,” *Physical Review*, vol. 115, pp. 485–491, Aug. 1959.
- [20] D. J. Thouless, M. Kohmoto, M. P. Nightingale, and M. den Nijs, “Quantized Hall Conductance in a Two-Dimensional Periodic Potential,” *Physical Review Letters*, vol. 49, pp. 405–408, Aug. 1982.
- [21] B. A. Bernevig, *Topological Insulators and Topological Superconductors*. Princeton University Press, stu - stud ed., 2013.

# Chapter 3

## Geometrical interpretations of Berry phase

*“Geometry draws the soul towards truth.”*

---

Plato

The previous chapter provided background on the key ideas we will be exploring in this paper in the context of spinor Bose-Einstein condensates in the following chapter. The underlying theme throughout is the use of geometry to improve our understanding of the dynamics. As such, this chapter focuses on more geometrical methods for understanding the Berry phase, connection and curvature. In particular, we geometrically derive expressions for the curvature and also derive expressions for the Berry phase of a spin-1 state in terms of the Berry phases of its 2 spin-1/2 states in the stellar representation. The main results in this chapter relate to spin-1 but it is instructive to first develop the spin-1/2 theory.

### 3.1 Berry curvature

We formalise the notation used in the previous chapter following [1]. In the stellar representation, a spin- $F$  spinor  $\chi$  is described by a fully symmetrised collection of  $2F$  spin-1/2 states, where each spin-1/2 state is parametrised in terms of two coordinates  $\Omega = (\theta, \phi)$  on the unit sphere.

In this representation,

$$|\chi\rangle = \frac{1}{N} \sum_{\{\sigma\}} \left( \prod_{i=1}^{2F} \otimes |\Omega_{\sigma_i}\rangle \right) = \frac{\sqrt{(2F)!}}{N} |\vec{\Omega}\rangle$$

where  $N$  is a normalisation constant, and the sum over  $\sigma$  runs over the  $(2F)!$  permutations of the  $2F$  labels for the spin-half parts. We also define  $|\vec{\Omega}\rangle$  as the unnormalised sum over permutations of the tensor product.

## 3.2 Berry phase

In this section, we prove the result that for a spin-1/2 state, the Berry phase can be interpreted as half the solid angle subtended by the closed curve. We do so in two ways - the second in a more geometrical way. This second method more easily generalises to higher spin.

**Theorem 3.2.1.** *The Berry phase for spin-1/2 is half the solid angle subtended by the curve.*

*Proof.* We start by considering the Berry curvature  $f_{ab} = \nabla \times A_a = \partial_a A_b - \partial_b A_a$ . We have  $a_a = i \langle \Omega | \partial_a | \Omega \rangle$ . We have that  $0 = \partial_a \langle \Omega | \Omega \rangle = (\partial_a \langle \Omega |) | \Omega \rangle + \langle \Omega | (\partial_a | \Omega \rangle)$ , so  $(\partial_a \langle \Omega |) | \Omega \rangle = - \langle \Omega | (\partial_a | \Omega \rangle)$ .

$$f_{ab} = i \partial_a \langle \Omega | \partial_b | \Omega \rangle - i \partial_b \langle \Omega | \partial_a | \Omega \rangle = i (\partial_a \langle \Omega |) (\partial_b | \Omega \rangle) - i (\partial_b \langle \Omega |) (\partial_a | \Omega \rangle)$$

We now introduce the projection operator  $P = |\Omega\rangle \langle \Omega|$  as well as its orthogonal complement  $Q = 1 - P = 1 - |\Omega\rangle \langle \Omega|$ , which satisfies  $Q |\Omega\rangle = 0$  for a normalised spinor. Thus  $0 = \partial_a (Q |\Omega\rangle)$ , so  $Q \partial_a |\Omega\rangle = -(\partial_a Q) |\Omega\rangle$ , and similarly for  $\langle \Omega|$ . Also, since  $Q$  is a projector,  $Q^2 = Q$ . From both of these results and  $\partial_a Q = -\partial_a P$  it follows that

$$\begin{aligned} f_{ab} &= i \partial_a \langle \Omega | Q Q \partial_b | \Omega \rangle - i \partial_b \langle \Omega | Q Q \partial_a | \Omega \rangle \\ &= i \langle \Omega | \partial_a Q \cdot \partial_b Q | \Omega \rangle - i \langle \Omega | \partial_b Q \cdot \partial_a Q | \Omega \rangle \\ &= i \langle \Omega | \partial_a P \cdot \partial_b P | \Omega \rangle - i \langle \Omega | \partial_b P \cdot \partial_a P | \Omega \rangle \\ &= i \text{tr} (P [\partial_a P, \partial_b P] P) \end{aligned}$$

where after the first line the derivatives are understood to act solely on the object immediately to their right (we have suppressed brackets for ease of notation). In the last step we have put the expression in basis-independent form. Everything so far is all independent of spin. We now specialise to spin-1/2. Since the Pauli matrices (with the identity) form a basis for our Hermitian space, we write our projector  $P = \frac{1}{2}(1 + \vec{n} \cdot \vec{\sigma})$ , with  $\vec{\sigma}$  the vector of Pauli matrices and  $\vec{n} = \langle \vec{\sigma} \rangle$  a unit vector.

Since  $\partial_a P = \frac{1}{2} \partial_a \vec{n} \cdot \vec{\sigma}$ , by cyclicity of the trace and the fact that  $P$  is a projector, we have

$$\begin{aligned} f_{ab} &= i \operatorname{tr} (P[\partial_a P, \partial_b P]P) = \frac{1}{4} i \operatorname{tr} (P^2[\partial_a \vec{n} \cdot \vec{\sigma}, \partial_b \vec{n} \cdot \vec{\sigma}]) \\ &= \frac{1}{4} i \operatorname{tr} (P(\partial_a \vec{n} \cdot \vec{\sigma} \partial_b \vec{n} \cdot \vec{\sigma} - \partial_b \vec{n} \cdot \vec{\sigma} \partial_a \vec{n} \cdot \vec{\sigma})) \end{aligned} \quad (3.1)$$

Using the well-known identity for vectors  $\vec{B}_1, \vec{B}_2$  that  $(\vec{B}_1 \cdot \sigma)(\vec{B}_2 \cdot \sigma) = \vec{B}_1 \cdot \vec{B}_2 I + i(\vec{B}_1 \times \vec{B}_2) \cdot \vec{\sigma}$ , we have

$$(\partial_a \vec{n} \cdot \vec{\sigma})(\partial_b \vec{n} \cdot \vec{\sigma}) = \partial_a \vec{n} \cdot \partial_b \vec{n} I + i(\partial_a \vec{n} \times \partial_b \vec{n}) \cdot \vec{\sigma}$$

Consequently, when expanding the commutator in equation (3.1), the dot products cancel, and the cross products reinforce, so we are left with

$$f_{ab} = -\frac{1}{2} \operatorname{tr} (P(\partial_a \vec{n} \times \partial_b \vec{n}) \cdot \sigma) = -\frac{1}{2} \operatorname{tr} ((I + \vec{n} \cdot \vec{\sigma})(\partial_a \vec{n} \times \partial_b \vec{n}) \cdot \vec{\sigma})$$

Applying the same identity again,

$$f_{ab} = -\frac{1}{2} \operatorname{tr} ((\partial_a \vec{n} \times \partial_b \vec{n}) \cdot \vec{\sigma} + \vec{n} \cdot (\partial_a \vec{n} \times \partial_b \vec{n}) I + \vec{n} \times (\partial_a \vec{n} \times \partial_b \vec{n}) \cdot \vec{\sigma})$$

The left-most term disappears because  $\operatorname{tr} \vec{a} \cdot \vec{\sigma} = 0$  for any  $\vec{a}$ . Expanding the right-most term vector triple product shows that this term disappears too. Thus finally

$$f_{ab} = -\vec{n} \cdot (\partial_a \vec{n} \times \partial_b \vec{n})$$

This is the area element, so the integration yields exactly what we require upon  $\vec{n} \mapsto \vec{n}/2$ .

□

We now tackle this problem more geometrically, following the method in [1], providing additional detail.

First, we construct an orthonormal basis  $\{\vec{e}_x, \vec{e}_y, \vec{n}\}$  for a given  $\vec{n}$ , where  $|\Omega\rangle$  is the highest value eigenvector of  $\vec{F} \cdot \vec{n}$ . Denote the time reversed state corresponding to  $|\Omega\rangle$  via  $|\Omega^t\rangle$  and note that by Kramer's Theorem  $\langle \Omega^t | \Omega \rangle = 0$ .

Define  $\vec{n} = 2 \langle \Omega | \vec{F} | \Omega \rangle$  and then states corresponding to 'x' and 'y' directions with respect to  $\vec{n}$  as  $|\Omega_x\rangle = \frac{1}{\sqrt{2}}(|\Omega\rangle + |\Omega^t\rangle)$  and  $|\Omega_y\rangle = \frac{1}{\sqrt{2}}(|\Omega\rangle + i|\Omega^t\rangle)$ . Using these states, we form  $\vec{e}_x = 2 \langle \Omega_x | \vec{F} | \Omega_x \rangle$  and  $\vec{e}_y = 2 \langle \Omega_y | \vec{F} | \Omega_y \rangle$ , which complete the orthonormal triad.

Finally, from these we construct  $\vec{e}_\pm = \vec{e}_x \pm i\vec{e}_y$ .

**Lemma 3.2.2.**  $\vec{F} \cdot \vec{e}_\pm$  act as raising and lower ladder operators:  $\vec{F} \cdot \vec{e}_+ |\Omega\rangle = 0, \vec{F} \cdot \vec{e}_+ |\Omega^t\rangle = |\Omega\rangle$  and  $\vec{F} \cdot \vec{e}_- |\Omega\rangle = |\Omega^t\rangle, \vec{F} \cdot \vec{e}_- |\Omega^t\rangle = 0$

*Proof.* This follows from a direct analogy with the angular momentum operators  $\vec{F} \cdot \vec{e}_x \mapsto \hat{S}_x, \vec{F} \cdot \vec{e}_y \mapsto \hat{S}_y, \vec{F} \cdot \vec{n} \mapsto \hat{S}_z$  □

**Lemma 3.2.3.**  $\frac{1}{2}\vec{e}_+ = \langle \Omega^t | \vec{F} | \Omega \rangle$

*Proof.* First write

$$\vec{F} = (\vec{F} \cdot \vec{n})\vec{n} + (\vec{F} \cdot \vec{e}_x)\vec{e}_x + (\vec{F} \cdot \vec{e}_y)\vec{e}_y = (\vec{F} \cdot \vec{n})\vec{n} + \frac{1}{2}(\vec{F} \cdot \vec{e}_+)\vec{e}_- + \frac{1}{2}(\vec{F} \cdot \vec{e}_-)\vec{e}_+$$

where the right hand side follows from expanding the definitions of  $\vec{e}_\pm$ . Using the ladder relations and acting with  $|\Omega\rangle$  and  $\langle \Omega^t |$  yields the result. □

**Lemma 3.2.4.**  $\vec{e}_x \cdot \partial_\alpha \vec{e}_y = -\vec{e}_y \cdot \partial_\alpha \vec{e}_x$

*Proof.* By orthogonality of  $\vec{e}_x$  and  $\vec{e}_y$ ,  $\partial_\alpha(\vec{e}_x \cdot \vec{e}_y) = 0 = \partial_\alpha \vec{e}_x \cdot \vec{e}_y + \vec{e}_x \cdot \partial_\alpha \vec{e}_y$  □

**Theorem 3.2.5.** For spin-1/2, the Berry connection  $a_\alpha = i \langle \Omega | \partial_\alpha \Omega \rangle = \frac{1}{2} \vec{e}_y \cdot \partial_\alpha \vec{e}_x$  and the curvature field tensor  $f_{\alpha\beta} = \partial_\alpha a_\beta - \partial_\beta a_\alpha = -\frac{1}{2} \vec{n} \cdot (\partial_\alpha \vec{n} \times \partial_\beta \vec{n})$

*Proof.* For the connection, use the ladder operators and apply the derivative to each term:

$$\partial_\alpha \langle \Omega | \Omega \rangle = \partial_\alpha (\langle \Omega^t | \vec{F} \cdot \vec{e}_- | \Omega \rangle) = \langle \partial_\alpha \Omega^t | \Omega^t \rangle + \langle \Omega^t | \vec{F} \cdot \partial_\alpha \vec{e}_- | \Omega \rangle + \langle \Omega | \partial_\alpha \Omega \rangle$$

Then

$$\langle \partial_\alpha \Omega^t | \Omega^t \rangle + \langle \Omega | \partial_\alpha \Omega \rangle = - \langle \Omega^t | \vec{F} \cdot \partial_\alpha \vec{e}_- | \Omega \rangle = - \langle \Omega^t | \vec{F} | \Omega \rangle \cdot \partial_\alpha \vec{e}_- = -\frac{1}{2} \vec{e}_+ \cdot \partial_\alpha \vec{e}_-$$

where we have used Lemma 3.2.3. Finally, since  $\langle \partial_\alpha \Omega^t | \Omega^t \rangle = \langle \Omega | \partial_\alpha \Omega \rangle$ , expanding  $\vec{e}_\pm$  in terms of  $\vec{e}_x$  and  $\vec{e}_y$  and using Lemma 3.2.4 yields the result.

Substituting this form of the connection into the curvature results in the cancellation of cross-derivatives and we get

$$f_{\alpha\beta} = \partial_\alpha a_\beta - \partial_\beta a_\alpha = \frac{1}{2} (\partial_\alpha \vec{e}_y \cdot \partial_\beta \vec{e}_x - \partial_\beta \vec{e}_y \cdot \partial_\alpha \vec{e}_x)$$

Since for a unit vector  $\vec{v}$  we have  $\vec{v} \cdot \partial \vec{v} = 0$ , using our triad we can write  $\partial_\alpha \vec{e}_y = \lambda_1 \vec{e}_x + \mu_1 \vec{n}$  and  $\partial_\beta \vec{e}_x = \lambda_2 \vec{e}_y + \mu_2 \vec{n}$ . By orthogonality,  $\partial_\alpha \vec{e}_y \cdot \partial_\beta \vec{e}_x = \mu_1 \mu_2 = (\partial_\alpha \vec{e}_y \cdot \vec{n})(\partial_\beta \vec{e}_x \cdot \vec{n})$ . Now since  $0 = \vec{e}_x \cdot \vec{n}$  we have  $\partial \vec{e}_x \cdot \vec{n} = -\vec{e}_x \cdot \partial \vec{n}$  so that

$$\begin{aligned} f_{\alpha\beta} &= \frac{1}{2} (\partial_\alpha \vec{e}_y \cdot \vec{n})(\partial_\beta \vec{e}_x \cdot \vec{n}) - \frac{1}{2} (\partial_\beta \vec{e}_y \cdot \vec{n})(\partial_\alpha \vec{e}_x \cdot \vec{n}) \\ &= \frac{1}{2} (\vec{e}_y \cdot \partial_\alpha \vec{n})(\vec{e}_x \cdot \partial_\beta \vec{n}) - \frac{1}{2} (\vec{e}_y \cdot \partial_\beta \vec{n})(\vec{e}_x \cdot \partial_\alpha \vec{n}) \\ &= \frac{1}{2} (\vec{e}_y \times \vec{e}_x) \cdot (\partial_\alpha \vec{n} \times \partial_\beta \vec{n}) \\ &= -\frac{1}{2} \vec{n} \cdot (\partial_\alpha \vec{n} \times \partial_\beta \vec{n}) \end{aligned}$$

where in the third equality we have used the vector identity 7.

□

### 3.2.1 Spin 1

We now develop similar results for the spin-1 case. We first present some lemmas and then build to the main result of the section. The below provide further detail to results in [1].

**Lemma 3.2.6.** *The overlap  $|\langle \Omega_1 | \Omega_2 \rangle|^2 = \frac{1 + \vec{n}_1 \cdot \vec{n}_2}{2}$  - this is a gauge independent result.*

*Proof.* With  $\vec{n}_i = (\sin \theta_i \cos \phi_i, \sin \theta_i \sin \phi_i, \cos \theta_i)^T$ , we have

$$\vec{n}_1 \cdot \vec{n}_2 = \sin \theta_1 \sin \theta_2 \cos(\phi_1 - \phi_2) + \cos \theta_1 \cos \theta_2$$

On the other hand, with  $|\Omega_i\rangle = \cos \frac{\theta_i}{2} e^{i\phi_i/2} |\uparrow\rangle + \sin \frac{\theta_i}{2} e^{-i\phi_i/2} |\downarrow\rangle$ , we have, with  $\Phi = \frac{\phi_2 - \phi_1}{2}$

$$\begin{aligned} \langle \Omega_1 | \Omega_2 \rangle &= \cos \frac{\theta_1}{2} \cos \frac{\theta_2}{2} e^{i\Phi} + \sin \frac{\theta_1}{2} \sin \frac{\theta_2}{2} e^{-i\Phi} \\ &= \cos \Phi \left( \cos \frac{\theta_1}{2} \cos \frac{\theta_2}{2} + \sin \frac{\theta_1}{2} \sin \frac{\theta_2}{2} \right) + i \sin \Phi \left( \cos \frac{\theta_1}{2} \cos \frac{\theta_2}{2} - \sin \frac{\theta_1}{2} \sin \frac{\theta_2}{2} \right) \end{aligned}$$

Now using  $\cos^2 \Phi + \sin^2 \Phi = 1$  and  $\cos^2 \Phi - \sin^2 \Phi = \cos 2\Phi$  we have (the gauge choice stops making a difference upon taking the magnitude)

$$\begin{aligned} |\langle \Omega_1 | \Omega_2 \rangle|^2 &= \cos^2 \frac{\theta_1}{2} \cos^2 \frac{\theta_2}{2} + \sin^2 \frac{\theta_1}{2} \sin^2 \frac{\theta_2}{2} + 2 \cos 2\Phi \cos \frac{\theta_1}{2} \cos \frac{\theta_2}{2} \sin \frac{\theta_1}{2} \sin \frac{\theta_2}{2} \\ &= \cos^2 \frac{\theta_1}{2} \cos^2 \frac{\theta_2}{2} + \sin^2 \frac{\theta_1}{2} \sin^2 \frac{\theta_2}{2} + \frac{1}{2} \cos(\phi_1 - \phi_2) \sin \theta_1 \sin \theta_2 \\ &= \frac{1 + \cos \theta_1}{2} \cdot \frac{1 + \cos \theta_2}{2} + \frac{1 - \cos \theta_1}{2} \cdot \frac{1 - \cos \theta_2}{2} + \frac{1}{2} \sin \theta_1 \sin \theta_2 \cos(\phi_1 - \phi_2) \\ &= \frac{1}{2} (1 + \vec{n}_1 \cdot \vec{n}_2) \end{aligned}$$

using trigonometric identities 3 and 4. □

Lemma 3.2.6 is used in the following result, which we quote from [1] without proof.

**Theorem 3.2.7.** *For spin 1 we have the results*

$$a_\alpha = \frac{1}{2} \vec{e}_{1y} \cdot \partial_\alpha \vec{e}_{1x} + \frac{1}{2} \vec{e}_{2y} \cdot \partial_\alpha \vec{e}_{2x} + \frac{1}{2} \frac{(\vec{n}_2 \times \vec{n}_1) \cdot \partial_\alpha \vec{n}_1 + (\vec{n}_1 \times \vec{n}_2) \cdot \partial_\alpha \vec{n}_2}{3 + \vec{n}_1 \cdot \vec{n}_2}$$

and

$$f_{\alpha\beta} = \frac{-2}{(3 + (\vec{n}_1 \cdot \vec{n}_2)^2)} \times (2\vec{n}_1 \cdot (\partial_\alpha \vec{n}_1 \times \partial_\beta \vec{n}_1) + 2\vec{n}_2 \cdot (\partial_\alpha \vec{n}_2 \times \partial_\beta \vec{n}_2) + (\vec{n}_1 + \vec{n}_2) \cdot (\partial_\alpha \vec{n}_1 \times \partial_\beta \vec{n}_2 + \partial_\alpha \vec{n}_2 \times \partial_\beta \vec{n}_1))$$

In particular, in the ferromagnetic state  $\vec{n} = \vec{n}_1 = \vec{n}_2$  this reduces to  $f_{\alpha\beta} = -\vec{n} \cdot (\partial_\alpha \vec{n} \times \partial_\beta \vec{n})$ .

In the nematic state  $\vec{n} = \vec{n}_1 = -\vec{n}_2$  the field tensor identically vanishes.

This says that the Berry connection for a spin-1 particle is the sum of its connections in the stellar representation as well as an interference term. We can thus determine situations in which the interference term disappears. The following results are discussed in [2].

**Corollary 3.2.7.1.** *If  $\partial_\alpha \vec{n}_1 = \partial_\alpha \vec{n}_2$  or  $(\vec{n}_1 \times \vec{n}_2) \cdot (\partial_\alpha \vec{n}_1 - \partial_\alpha \vec{n}_2)$  then  $a_\alpha = a_{1\alpha} + a_{2\alpha}$ , that is, the overall Berry connection is the sum of the individual connections. The first case corresponds to a rigid rotation of the great circle connecting  $\vec{n}_1$  and  $\vec{n}_2$ ; the second corresponds to  $\vec{n}_1$  and  $\vec{n}_2$  sliding along the great circle connecting them (this includes the case of  $\vec{n}_1 = \pm \vec{n}_2$ ).*

*Proof.* This is immediate upon rewriting

$$a_\alpha = a_{1\alpha} + a_{2\alpha} - \frac{1}{2(3 + \vec{n}_1 \cdot \vec{n}_2)} ((\vec{n}_1 \times \vec{n}_2) \cdot (\partial_\alpha \vec{n}_1 - \partial_\alpha \vec{n}_2))$$

□

This relationship between the connections can be used to deduce a relationship between the Berry phases. In order to do so, we reinterpret the interference term as per Lemma 3.2.8.

**Lemma 3.2.8.** *With the barycenter  $\vec{R} = \frac{1}{2}(\vec{n}_1 + \vec{n}_2)$  and the difference  $\vec{r} = \vec{n}_1 - \vec{n}_2$  we have*

$$a_\alpha = a_{1\alpha} + a_{2\alpha} + C(\Theta) \cos \Theta \hat{R} \cdot (\hat{r} \times \partial_\alpha \hat{r})$$

where  $C(x) = \sin^2 x / (1 + \cos^2 x)$ ,  $2\Theta = \arccos \vec{n}_1 \cdot \vec{n}_2$  is the angle between the two normals and the hat denotes the unit vector.

*Proof.* Note first that  $\vec{R} \cdot \vec{R} = \frac{1}{2}(1 + \vec{n}_1 \cdot \vec{n}_2)$ ,  $\vec{r} \cdot \vec{r} = 2(1 - \vec{n}_1 \cdot \vec{n}_2)$  and  $\vec{R} \times \vec{r} = \vec{n}_2 \times \vec{n}_1$ . Also, by trigonometric identities (1) and (2) we have

$$C(\Theta) \cos \Theta = \frac{\frac{1 - \cos 2\Theta}{2}}{1 + \frac{1 + \cos 2\Theta}{2}} \sqrt{\frac{1 + \cos 2\Theta}{2}} = \frac{1 - \vec{n}_1 \cdot \vec{n}_2}{3 + \vec{n}_1 \cdot \vec{n}_2} \sqrt{\frac{1 + \vec{n}_1 \cdot \vec{n}_2}{2}}$$

Consequently,

$$\begin{aligned} -\frac{1}{2(3 + \vec{n}_1 \cdot \vec{n}_2)} ((\vec{n}_1 \times \vec{n}_2) \cdot (\partial_\alpha \vec{n}_1 - \partial_\alpha \vec{n}_2)) &= \frac{1}{2(3 + \vec{n}_1 \cdot \vec{n}_2)} (\vec{n}_2 \times \vec{n}_1) \cdot \partial_\alpha \vec{r} \\ &= \frac{1}{(1 - \vec{n}_1 \cdot \vec{n}_2) \sqrt{2(1 + \vec{n}_1 \cdot \vec{n}_2)}} C(\Theta) \cos \Theta (\vec{R} \times \vec{r}) \cdot \partial_\alpha \vec{r} \\ &= C(\Theta) \cos \Theta \hat{R} \cdot (\hat{r} \times \partial_\alpha \hat{r}) \end{aligned}$$

□

Finally, identifying

$$\hat{R} \cdot (\hat{r} \times \partial_\alpha \hat{r}) = d\phi$$

yields an expression for the Berry phase

$$\gamma = \gamma_1 + \gamma_2 + \oint C(\Theta) \cos \Theta d\phi \quad (3.2)$$

With this expression, we can determine when the Berry phase simplifies in terms of the Berry phase of its Majorana stars.

**Corollary 3.2.8.1.** *When the angle between the normals is  $2\Theta = \arccos \alpha$ , the Berry phase is*

$$\gamma = \gamma_1 + \gamma_2 + \frac{1 - \alpha^2}{1 + \alpha^2} \sqrt{\frac{1 + \alpha}{2}} \oint d\phi$$

*Proof.* This follows from evaluating  $C(\Theta) \cos \Theta$  with  $2\Theta = \arccos \alpha$  in equation (3.2) □

**Corollary 3.2.8.2.** *When  $\vec{n}_1 \cdot \vec{n}_2 = \pm 1$  the Berry phase is exactly the Berry phase of the individual stars.*

*Proof.* This follows immediately from Corollary 3.2.8.1. □

## References

- [1] R. Barnett, D. Podolsky, and G. Refael, “Geometrical approach to hydrodynamics and low-energy excitations of spinor condensates,” *Physical Review B - Condensed Matter and Materials Physics*, vol. 80, no. 2, 2009.
- [2] C. Kam and R. B. Liu, “Berry phases of higher spins due to internal geometry of Majorana constellation and relation to quantum entanglement,” 2020.

# Chapter 4

## Bose-Einstein condensates

*“Assume a spherical cow...”*

---

Unknown

Few phenomena demonstrate the rapid recent advances of condensed matter physics as well as Bose-Einstein condensates. A mainstay in classical statistical mechanics education as a niche phase of matter, BECs were only experimentally realised relatively recently. Seminal works in 1998 by Ho [1] and Ohmi and Machida [2] paved the way for a wave of developments over the last two decades.

In this section we provide a brief introduction to the dynamics of spinor BECs. For the sake of brevity, the full development is not presented. Further detail can be found in the numerous references provided. The first part of this chapter provides an introduction to the phenomenon of Bose-Einstein condensation. In the second part we analyse the spin-1 equations of motion. Here we use the results from the previous chapters to understand the Majorana dynamics and relate the Berry phase of the spin-1 states to that of the spin-1/2 states. In the final part, we provide a brief overview of some of the richer dynamics in the spin-2 system. Apart from the background material, the results in this chapter are entirely original.

## 4.1 Introduction

BECs are a quantum statistical phenomenon first predicted by Einstein in 1925 [3], building on ideas by Bose on the statistics of photons [4] (hence the name). Consider an ensemble of  $N$  macroscopic bosons<sup>1</sup>. For suitable systems below the so-called *transition temperature*, a macroscopic fraction of particles can occupy the same quantum ground state. This leads to many interesting properties, for example, the density at the centre of a BEC is many orders of magnitude lower than for a liquid or gas, and BECs can also form vortices. However, this comes at a cost - these systems can only be realised for temperatures of order  $10^{-5}K$  or less, and so are inherently extremely unstable. Note that the condensation<sup>2</sup> occurs for both interacting and non-interacting systems (although non-interacting systems are impossible to physically arrange). Further properties are outlined in [5] and a more detailed discussion can be found in [6].

There is an important distinction between spinor and scalar BECs. When a BEC is trapped in a magnetic potential, the spin aligns along the direction of a local magnetic field. Accordingly, the integral degrees of freedom are frozen, and the condensate is described by a scalar order parameter. On the other hand, when trapped in an optical potential, the internal degrees of freedom are not frozen. The order parameter is thus a spinor, and such condensates are called *spinor Bose-Einstein condensates* [6]. These are the condensates that we will analyse in the remainder of this chapter.

In the quantum mechanical description of BECs, the condensate wave function is often referred to as the *order parameter*, based on the thermodynamic definition of an order parameter as a quantity which changes value to uniquely classify phase transitions. It can be shown that the condensate wave function is a thermodynamic quantity that appears in the thermodynamic limit [6] and thus the macroscopic wavefunction describes coherent properties of a many-body system without referring to its microscopic details.

In 1995, the first Bose-Einstein condensates were created using atoms in a single spin state of rubidium-87 [7] and of sodium-23 [8]. Shortly afterwards, in 1997, lithium-7 was also realised

---

<sup>1</sup>Recall that by the spin-statistics theorem, bosons are particles with integer spin and fermions are particles with half-integer spin. By the Pauli exclusion principle, bosons can occupy the same energy state, but fermions cannot.

<sup>2</sup>Condensation here refers to the phenomena of a *macroscopic* number of bosons occupying the same *microscopic* quantum state

[9]. In these systems, only those atoms in a weak-field seeking state were magnetically trapped - these were scalar BECs as their spin degrees of freedom were frozen [6]. The first spinor BEC was realised in a gas of spin-1 sodium-23 atoms confined in an optical dipole trap in 1998 [10], opening up a new research arena of ultracold atomic systems. Since the earliest experiments, many more atoms have been demonstrated to undergo Bose-Einstein condensation [11].

There are many fascinating applications of BECs. A link between superfluidity and BECs was first suggested by Fritz London in 1938 [12]. In 1999, BECs were used to slow down light pulses to speeds as low as 17 metres per second (approximately 38 kilometres per hour). On the other hand, just last year, a BEC of rubidium atoms was created and observed in freefall for over a second on board the International Space Station [13]!

## 4.2 Spin 1

Consider two hyperfine spin-1 bosons in the absence of both linear and quadratic Zeeman effects. Addition of two spin 1 particles can result in a total spin of 0, 1 or 2, but since we are considering bosons we are restricted to symmetrised states. The spin 1 states are antisymmetric [6], so the total spin is either 0 or 2. As shown in [1], the general form of the low energy interaction is  $V = g_0\mathcal{P}_0 + g_2\mathcal{P}_2$ , where  $g_i = 4\pi\hbar^2 a_F/M$  characterises the strength of the interaction between two particles with total spin  $F$ , depending on  $M$  the mass of the atom and  $a_F$  the  $s$ -wave scattering length in the total spin- $F$  channel;  $\mathcal{P}_F$  the projection operator projecting the pair into a total hyperfine spin  $F$  state. Noting that the eigenvalues of  $\vec{F}_1 \cdot \vec{F}_2$  are -2 for spin 0 and 1 for spin 2, the projection operators are

$$P_0 = (2 + \vec{F}_1 \cdot \vec{F}_2), P_2 = (-1 + \vec{F}_1 \cdot \vec{F}_2)$$

Thus, we may write

$$g_0P_0 + g_2P_2 = c_0 + c_1\vec{F}_1 \cdot \vec{F}_2 \text{ where } c_0 = \frac{g_0 + 2g_2}{3}, c_1 = \frac{g_2 - g_0}{3}$$

This form of the potential leads to<sup>3</sup> (using the summation convention)

---

<sup>3</sup>Some details have been skipped for brevity - the full calculation requires minimising the energy functional

$$i\hbar \frac{\partial \psi_m}{\partial t} = \left( \frac{p^2}{2m} + c_0 \psi_a^\dagger \psi_a \right) \psi_m + c_1 \psi_a^\dagger \vec{F}_{ab} \psi_b \cdot [\vec{F} \psi]_m$$

This is the Gross-Pitaevskii equation, the general equation of motion for a spin 1 spinor (Bose-Einstein) condensate with no (linear or quadratic) Zeeman effects or potential. Significant work has been done on understanding these systems in optical and magnetic traps, and indeed more general systems for higher spins [14, 15, 16]. Since our goal here is to focus on the Majorana representation, we will simplify the problem further by using the *single mode approximation* (SMA), where we assume that all atoms share the same spatial order parameter. Although generally a useful approximation, the SMA is not entirely exact. For an investigation into validity conditions, see [17]. A treatment beyond the single mode approximation can be found in [18].

In the SMA we write the 3D order parameter as  $\psi_m(x, t) = \phi_m(x, t)\chi$  to find

$$\chi \left( i\hbar \frac{\partial}{\partial t} - \frac{p_x^2}{2m} \right) \phi_m = \phi_m \left( c_0 |\phi|^2 |\chi|^2 + \frac{c_1}{\phi_m} |\chi|^2 \phi_a^\dagger \vec{F}_{ab} \phi_b \cdot [\vec{F} \phi]_m \right) \chi$$

For this equality to hold, we require the right hand bracket to be equal to a functional  $\mu(\phi_m)$ .

Then

$$\chi \left( i\hbar \frac{\partial}{\partial t} - \frac{p_x^2}{2m} \right) \phi_m = \phi_m \mu(\phi_m) \chi$$

Finally, ignoring spatial dependences we arrive at

$$i\hbar \frac{\partial \phi_m}{\partial t} = c_0 \phi_m + c_1 \phi_a^\dagger \vec{F}_{ab} \phi_b \cdot [\vec{F} \phi]_m$$

for a normalised spinor.

### 4.2.1 Dynamics

We now consider time evolution on the Majorana sphere. The  $c_0$  term does not affect the Majorana dynamics; it can be removed via a global change of phase  $\phi_m \mapsto \phi_m e^{i\hbar c_0 t}$ . Since the

---

$E[\psi] = \langle \hat{H} \rangle$ . See [6] for full details

motion is independent of  $c_0$ , we can take it as 0. The dynamics in this regime therefore do not tell us what  $c_0$  is, since we are just looking at the spinor motion and not the phase. Then, in units where  $\hbar = 1$ , with  $\vec{m} = \langle \vec{S} \rangle = (m_1, m_2, m_3)^T$ , the system reduces to (writing the system in terms of  $\psi$  as per convention)

$$i \frac{\partial \psi}{\partial t} = c_1 \langle \vec{S} \rangle \cdot \vec{S} \psi = c_1 \vec{m} \cdot \vec{S} \psi \quad (4.1)$$

**Theorem 4.2.1.**  $\vec{m}$  is a constant of motion.

*Proof.* Using Heisenberg's equations of motion, we have

$$\dot{\vec{m}} = i \langle [H, \vec{S}] \rangle \implies \dot{m}_i = i \langle [H, S_i] \rangle$$

Thus, by repeatedly using the canonical commutation relations  $[S_i, S_j] = i\epsilon_{ijk}S_k$ , we have

$$\begin{aligned} \dot{m}_1 &= i \langle [m_1 S_1 + m_2 S_2 + m_3 S_3, S_1] \rangle = i \langle m_2 [S_2, S_1] + m_3 [S_3, S_1] \rangle \\ &= i \langle m_2 [S_2, S_1] + m_3 [S_3, S_1] \rangle = i \langle -im_2 S_3 + im_3 S_2 \rangle \\ &= m_2 \langle S_3 \rangle - m_3 \langle S_2 \rangle = m_2 m_3 - m_3 m_2 = 0 \end{aligned}$$

and similarly  $\dot{m}_2 = \dot{m}_3 = 0$ . It follows that  $\dot{\vec{m}} = 0$ . □

**Corollary 4.2.1.1.** The solution to equation (4.1) is  $\psi(t) = \exp(-ic_1 \vec{m} \cdot \vec{S} t) \psi(0)$ . The time period for the stellar representation is given by

$$T = \frac{2\pi}{c_1 |\vec{m}|}$$

Note that  $|\vec{m}|$  is not necessarily 1.

**Corollary 4.2.1.2.** In the Majorana representation,  $\vec{n}_1 + \vec{n}_2$  and  $\vec{n}_1 \cdot \vec{n}_2$  are constants of motion. These correspond to the direction of alignment and radius of a circle on the unit sphere, respectively.

*Proof.* The conservation of  $\vec{m}$  (the expectation of  $\vec{S}$ ) tells us that the spin is polarised in a

certain direction, but by dimensionality arguments for spin-1, conservation of  $\vec{m}$  is not sufficient to determine the spinor (in contrast to spin-1/2). However, it tells us that on average, the spin points in the same direction. Thus, as the length of the  $\vec{n}_i$  is fixed, the angle between the two normals and the barycenter are constants of the motion.  $\square$

To understand the dynamics of this system, consider first eigenstates of the operator  $\vec{m} \cdot \vec{S}$ . These will be stationary in the Majorana representation as the spinor is unchanged up to normalisation. However, this operator has a 0 eigenvalue whose corresponding eigenstates behave slightly differently from the non-0 eigenvalues.

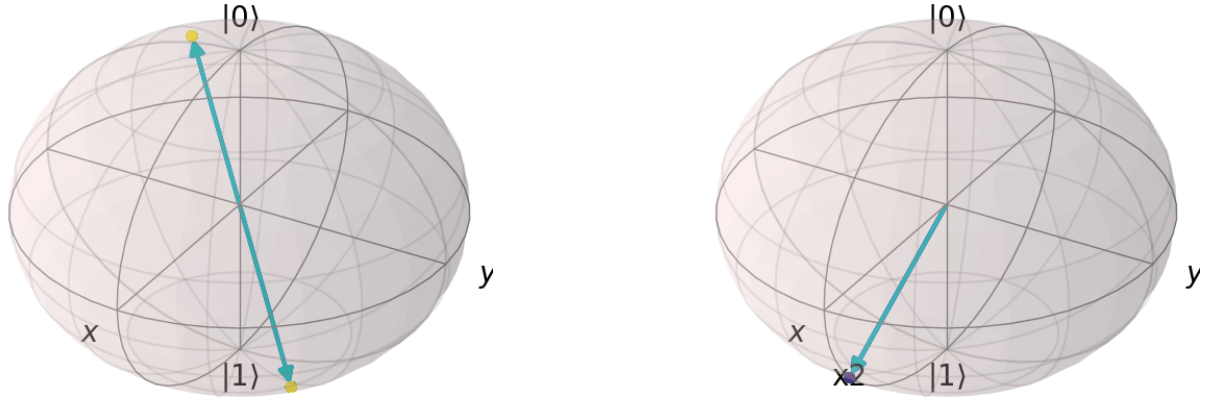
The 0 energy eigenstate is given by  $(-m_1 + im_2, m_3, m_1 + im_2)^T$ . Writing  $m_1 + im_2 = re^{-i\phi}$  (the reason for the minus sign will become clear shortly) the 0 energy eigenstate is equivalently  $(1, -\frac{m_3}{r}e^{-i\phi}, -e^{-2i\phi})$ . This is exactly the form of the antipodal points in Corollary 2.2.3.1. Conversely, a quick computation shows that antipodal points satisfy  $\vec{m} = 0$ , and so the Majorana representation is completely stationary. On the other hand, eigenstates with non-zero energy can be identified with repeated roots. Figure 4.1 shows the (constant) time evolution of eigenstates.

These results match what we expect - recall that the Majorana representation is constructed such that the eigenstates of  $\vec{m} \cdot \vec{S}$  are polarised in a specific direction. That the condensate system reduces to this is a coincidence that does not occur in higher spin.

Note that  $\vec{m} = 0$  if and only if  $\vec{m} \cdot \vec{S} = 0$ . There are thus two qualitatively different situations when  $\vec{m} = 0$  and when  $\vec{m} \neq 0$ . In the latter case, we have a defined (non-zero) direction of the expectation value of the spin. We see a circle on the sphere and non-trivial dynamics. On the other hand, when  $\vec{m} = 0$ , the Majorana representation points in opposite directions:  $\vec{n}_1 = -\vec{n}_2$ . There is no evolution on the sphere since the right hand side of the differential equation is now identically 0.

On the other hand, when the initial state  $\psi(0)$  is not an eigenstate, we observe circles on the sphere. Figure 4.3 shows the time evolution of two example states.

We can also relate these results to ground states. To find the ground state we want to minimise  $c_1 \langle \vec{S} \rangle^2$ . If  $c_1 > 0$ , we want to minimise  $\langle \vec{S} \rangle^2$ , namely choosing the zero eigenstate, which enforces  $\langle \vec{S} \rangle^2 = 0$ , which corresponds to antipodal points (the polar state). On the other



(a) Zero energy eigenstate  $\psi = (-3 + 3i, 4, 3 + 3i)$

(b) Non-zero energy eigenstate  $\psi = (1, -1 - \sqrt{3}, 2 + \sqrt{3})$

Figure 4.1: Time evolution of eigenstates of  $\vec{m} \cdot \vec{S}$  under  $c_0 = 0$

hand, if  $c_1 < 0$ , we want to maximise  $\langle \vec{S} \rangle^2$ , which corresponds to the negative eigenstate (the ferromagnetic state). This matches the results in Ho's seminal paper [1].

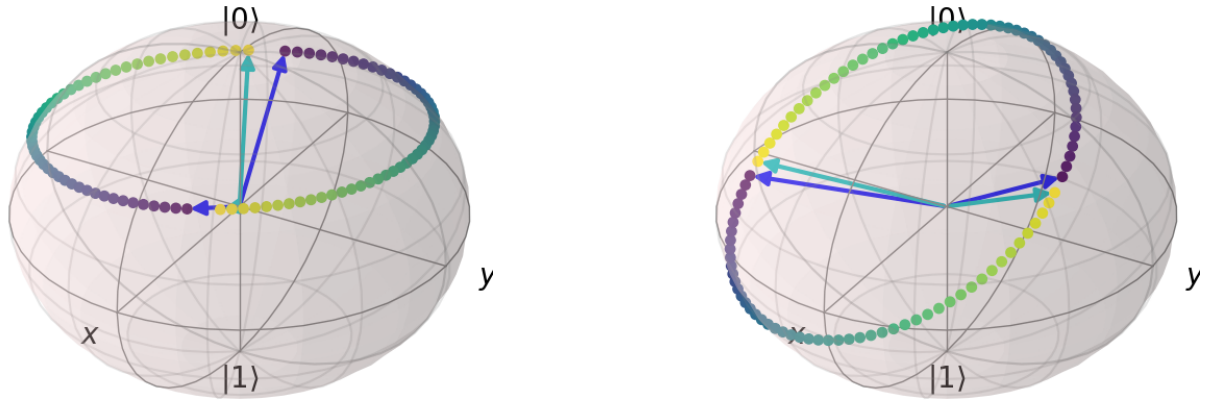
In summary, the dynamics yield either stationary normals or circles on the sphere. A higher coefficient  $c_1$  results in higher frequency. If the time period can be measured for a given initial condition  $\psi(0)$ , we can calculate  $c_1$  and therefore the scattering length. The time period for the Majorana representation can be computed by observing components of the spinor  $|\psi_1|^2, |\psi_0|^2, |\psi_{-1}|^2$  and calculating the representation at each timestep.

To close this discussion, we recast the dynamics in terms of the normal vectors. Recall that for a spin-1/2 system with Hamiltonian  $\hat{H} = \vec{B} \cdot \vec{\sigma}$ , where  $\vec{\sigma}$  is the Pauli vector, we can reinterpret this system geometrically. With  $\vec{m} = \langle \psi | \vec{\sigma} | \psi \rangle$ , a quick computation shows that  $\dot{\vec{m}} = 2\vec{B} \times \vec{m}$ .

We may similarly interpret the dynamics for the condensate in terms of the normals  $\vec{n}_i$ . The mean field spin 1 equations of motion reduce to the coupled system

$$\dot{\vec{n}}_1 = (\vec{n}_1 + \vec{n}_2) \times \vec{n}_1 = \vec{n}_2 \times \vec{n}_1$$

$$\dot{\vec{n}}_2 = (\vec{n}_1 + \vec{n}_2) \times \vec{n}_2 = \vec{n}_1 \times \vec{n}_2$$


 (a)  $\psi(0) = (5, 5 + 5i, 1)$ 

 (b)  $\psi(0) = (3 + 3i, -2 + i, 2 + i)$ 

Figure 4.2: Time evolution of states with given initial conditions under  $c_0 = 0$ . Purple is the start of the trajectory, yellow is the end.

subject to the initial conditions given from  $\psi(0)$ . From this, it follows immediately that  $\vec{n}_1 + \vec{n}_2$  is constant and that if the normals are (anti)parallel, they remain fixed. That is, if  $\vec{n} = \vec{n}_1 = \pm \vec{n}_2$ , then  $\dot{\vec{n}} = 0$ . Alternatively, this motion can be interpreted as circles of 0 radius.

### 4.2.2 Berry phase

Using our results from this chapter and the previous chapter, we can calculate the Berry phase for states under the spin-1 dynamics.

For eigenstates,  $\vec{n}_1 \cdot \vec{n}_2 = \pm 1$ , so we can express the Berry phase of the original spinor solely in terms of the Berry phase of its stars:

$$\gamma = \gamma_1 + \gamma_2 \quad (4.2)$$

For the zero energy eigenstate with antipodal points, if at the end of the cycle the points return to their original states, the Berry phase is 0, and if the antipodes permute, the Berry phase is -1 [19].

More generally, since the angle between the normals is preserved under these dynamics, by Corollary 3.2.8.1 the Berry phase of the spin-1 state can be expressed as

$$\gamma = \gamma_1 + \gamma_2 + \frac{1 - \alpha^2}{1 + \alpha^2} \sqrt{\frac{1 + \alpha}{2}} \oint d\phi$$

where  $\arccos \alpha$  is the angle between the normals. This reduces to equation (4.2) when  $\alpha = 0$ .

### 4.3 Spin 2

In a similar manner to the previous section, the spin 2 equations of motion can be derived. The total spin can now be 0, 1 or 2. The completeness relation for the projection operators is  $\mathcal{P}_0 + \mathcal{P}_2 + \mathcal{P}_4 = 1$ , and the eigenvalues of  $\vec{F}_1 \cdot \vec{F}_2$  are 0, 6 or 20 for  $F = 0, 1, 2$  respectively. Thus, after expressing the potential  $V = g_0\mathcal{P}_0 + g_2\mathcal{P}_2 + g_4\mathcal{P}_4$  in terms of  $\vec{F}_1 \cdot \vec{F}_2$  and  $\mathcal{P}_0$  and minimising the energy functional, the equations of motion are [6]

$$\begin{aligned} i\hbar \frac{\partial \psi_{\pm 2}}{\partial t} &= (c_0 \pm 2c_1 \langle f_z \rangle) \psi_{\pm 2} + c_1 \langle f_{\mp} \rangle \psi_{\pm 1} + \frac{c_2}{\sqrt{5}} A \psi_{\mp 2}^* \\ i\hbar \frac{\partial \psi_{\pm 1}}{\partial t} &= (c_0 \pm c_1 \langle f_z \rangle) \psi_{\pm 1} + c_1 \left( \frac{\sqrt{6}}{2} \langle f_{\mp} \rangle \psi_0 + \langle f_{\pm} \rangle \psi_{\pm 2} \right) - \frac{c_2}{\sqrt{5}} A \psi_{\mp 1}^*, \\ i\hbar \frac{\partial \psi_0}{\partial t} &= c_0 \psi_0 + \frac{\sqrt{6}}{2} c_1 (\langle f_+ \rangle \psi_1 + \langle f_- \rangle \psi_{-1}) + \frac{c_2}{\sqrt{5}} A \psi_0^* \end{aligned}$$

where

$$\begin{aligned} \langle f_+ \rangle &= \langle f_- \rangle^* = 2(\psi_2^* \psi_1 + \psi_{-1}^* \psi_{-2}) + \sqrt{6}(\psi_1^* \psi_0 + \psi_0^* \psi_{-1}) \\ \langle f_z \rangle &= 2(|\psi_2|^2 - |\psi_{-2}|^2) + |\psi_1|^2 - |\psi_{-1}|^2 \\ A &= \frac{1}{\sqrt{5}}(2\psi_2 \psi_{-2} - 2\psi_1 \psi_{-1} + \psi_0^2) \end{aligned}$$

This system is significantly more complicated than the spin-1 system and as such a full analysis is not provided in this paper. Instead, we focus solely on the case  $c_1 = 0$ . This is an unphysical limit but future work can build on this by interpreting the dynamics of the  $c_1$  term as deviations from this limiting behaviour. In the limit  $c_1 = 0$ , this system reduces to

$$\begin{aligned} i\hbar \frac{\partial \psi_{\pm 2}}{\partial t} &= c_0 \psi_{\pm 2} + \frac{c_2}{\sqrt{5}} A \psi_{\mp 2}^* \\ i\hbar \frac{\partial \psi_{\pm 1}}{\partial t} &= c_0 \psi_{\pm 1} - \frac{c_2}{\sqrt{5}} A \psi_{\mp 1}^*, \\ i\hbar \frac{\partial \psi_0}{\partial t} &= c_0 \psi_0 + \frac{c_2}{\sqrt{5}} A \psi_0^* \end{aligned}$$

or equivalently

$$i\hbar \frac{\partial \psi_m}{\partial t} = c_0 \psi_m + (-1)^m A \frac{c_2}{\sqrt{5}} \psi_{-m}^*$$

As before, the  $c_0$  term does not contribute to the Majorana dynamics as it can be removed via a gauge choice. Thus, in units where  $\hbar = 1$ , we arrive at

$$i \frac{\partial \psi_m}{\partial t} = (-1)^m A \frac{c_2}{\sqrt{5}} \psi_{-m}^*$$

**Lemma 4.3.1.** *The magnitude of  $A$  is a constant of the motion.*

*Proof.* Note that (with  $\hbar = 1$ )  $A$  satisfies

$$\begin{aligned} i\dot{A} &= \frac{1}{\sqrt{5}} (2i\dot{\psi}_2\psi_{-2} + 2i\psi_2\dot{\psi}_{-2} - 2i\dot{\psi}_1\psi_{-1} - 2i\psi_1\dot{\psi}_{-1} + 2i\dot{\psi}_0\psi_0) \\ &= \frac{1}{\sqrt{5}} \left( 2(c_0\dot{\psi}_2 + A \frac{c_2}{\sqrt{5}} \dot{\psi}_{-2}^*)\psi_{-2} + 2(c_0\dot{\psi}_{-2} + A \frac{c_2}{\sqrt{5}} \dot{\psi}_2^*)\psi_2 \right. \\ &\quad \left. - 2(c_0\dot{\psi}_1 - A \frac{c_2}{\sqrt{5}} \dot{\psi}_{-1}^*)\psi_{-1} - 2(c_0\dot{\psi}_{-1} - A \frac{c_2}{\sqrt{5}} \dot{\psi}_1^*)\psi_1 + 2\psi_0(c_0\dot{\psi}_0 + A \frac{c_2}{\sqrt{5}} \dot{\psi}_0^*) \right) \\ &= \frac{1}{\sqrt{5}} (2c_0(2\psi_2\dot{\psi}_{-2} - 2\psi_1\dot{\psi}_{-1} + \dot{\psi}_0^2) + \frac{2c_2}{\sqrt{5}} A (|\dot{\psi}_{-2}^2 + |\dot{\psi}_2|^2 + |\dot{\psi}_{-1}|^2 + |\dot{\psi}_1|^2 + |\dot{\psi}_0|^2)) \\ &= \frac{2}{\sqrt{5}} A \left( c_0 + \frac{c_2}{\sqrt{5}} \right) \end{aligned}$$

It follows that

$$A(t) = A(0) \exp \left( -it \left( \frac{2}{\sqrt{5}} \left( c_0 + \frac{c_2}{\sqrt{5}} \right) \right) \right)$$

In particular, the magnitude of  $A$  is constant. □

**Corollary 4.3.1.1.** *When  $A(0) = 0$ , the Majorana dynamics are fixed.*

*Proof.* This follows immediately since the magnitude of  $A$  is conserved. □

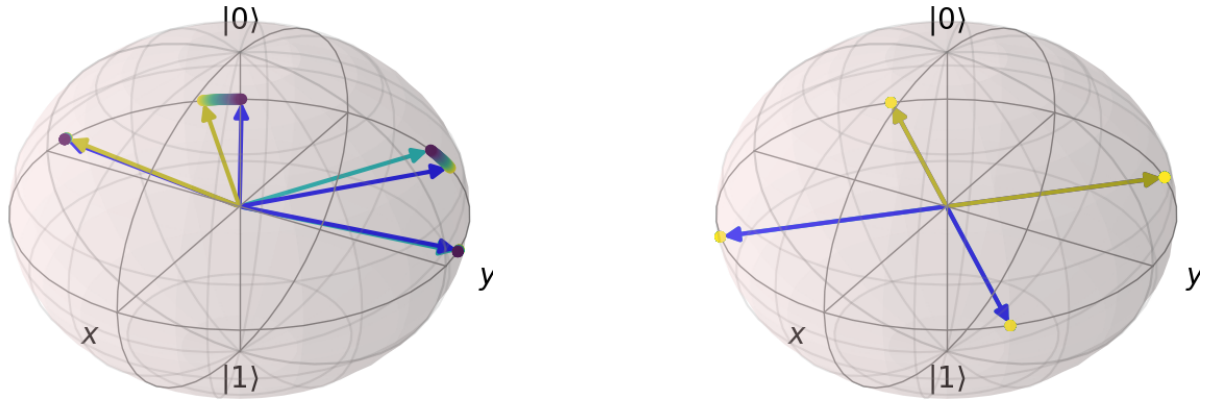
(a)  $\psi(0) = (1, 1, 1, 1, 1)$ (b)  $\psi(0) = (1, 0, 0, 0, 1)$ 

Figure 4.3: Time evolution of states with given initial conditions. Purple is the start of the trajectory, yellow is the end. On the left, the state is symmetric about the  $x$  axis and the dynamics are confined to the region  $y < 0$ . On the right, the dynamics are trivially stationary.

## References

- [1] T. L. Ho, “Spinor bose condensates in optical traps,” *Physical Review Letters*, vol. 81, no. 4, pp. 742–745, 1998.
- [2] T. Ohmi and K. Machida, “Bose-Einstein condensation with internal degrees of freedom in alkali atom gases,” *Journal of the Physical Society of Japan*, vol. 67, pp. 1822–1825, Nov. 1998.
- [3] A. Einstein, “Quantum Theory of a Monoatomic Ideal Gas A translation of Quantentheorie des einatomigen idealen Gases ( Einstein , 1924 ),” *Sitzungsberichte der Preuss. Akad. der Wissenschaften*, vol. 1, no. 3, 1925.
- [4] Bose, “Plancks Gesetz und Lichtquantenhypothese,” *Zeitschrift für Physik*, vol. 26, no. 1, pp. 178–181, 1924.
- [5] C. J. Pethick and H. Smith, *Bose–Einstein condensation in dilute gases*. Cambridge University Press, 2 ed., Jan. 2008.
- [6] M. Ueda, *Fundamentals and new frontiers of Bose-Einstein condensation*. World Scientific Publishing Co., Jan. 2010.

- [7] M. H. Anderson, J. R. Ensher, M. R. Matthews, C. E. Wieman, and E. A. Cornell, “Observation of Bose-Einstein Condensation in a Dilute Atomic Vapor,” *Science*, vol. 269, pp. 198 LP – 201, July 1995.
- [8] K. B. Davis, M. O. Mewes, M. R. Andrews, N. J. van Druten, D. S. Durfee, D. M. Kurn, and W. Ketterle, “Bose-Einstein Condensation in a Gas of Sodium Atoms,” *Physical Review Letters*, vol. 75, pp. 3969–3973, Nov. 1995.
- [9] C. C. Bradley, C. A. Sackett, and R. G. Hulet, “Bose-Einstein Condensation of Lithium: Observation of Limited Condensate Number,” *Physical Review Letters*, vol. 78, pp. 985–989, Feb. 1997.
- [10] D. M. Stamper-Kurn, M. R. Andrews, A. P. Chikkatur, S. Inouye, H.-J. Miesner, J. Stenger, and W. Ketterle, “Optical Confinement of a Bose-Einstein Condensate,” *Physical Review Letters*, vol. 80, pp. 2027–2030, Mar. 1998.
- [11] Y. Kawaguchia and M. Uedaa, “Spinor Bose-Einstein condensates,” *Physics Reports*, vol. 520, no. 5, pp. 253–381, 2012.
- [12] F. London, “On the Bose-Einstein Condensation,” *Physical Review*, vol. 54, pp. 947–954, Dec. 1938.
- [13] D. C. Aveline, J. R. Williams, E. R. Elliott, C. Dutenhoffer, J. R. Kellogg, J. M. Kohel, N. E. Lay, K. Oudrhiri, R. F. Shotwell, N. Yu, and R. J. Thompson, “Observation of Bose-Einstein condensates in an Earth-orbiting research lab,” *Nature*, vol. 582, no. 7811, pp. 193–197, 2020.
- [14] C. Trallero-Giner, R. Cipolatti, and T. C. H. Liew, “One-dimensional cubic-quintic Gross-Pitaevskii equation for Bose-Einstein condensates in a trap potential,” *The European Physical Journal D*, vol. 67, no. 7, 2013.
- [15] C. Trallero-Giner, D. G. Santiago-Pérez, V. Romero-Rochin, and G. E. Marques, “Collective modes of trapped spinor Bose-Einstein condensates,” *Journal of Physics B: Atomic, Molecular and Optical Physics*, vol. 50, no. 21, pp. 1–7, 2017.

- [16] C. K. Law, H. Pu, and N. P. Bigelow, “Quantum spins mixing in spinor bose-einstein condensates,” *Physical Review Letters*, vol. 81, pp. 5257–5261, Dec. 1998.
- [17] S. Yi, E. Müstecaplıođlu, C. P. Sun, and L. You, “Single-mode approximation in a spinor-1 atomic condensate,” *Physical Review A - Atomic, Molecular, and Optical Physics*, vol. 66, p. 4, July 2002.
- [18] J. Jie, Q. Guan, S. Zhong, A. Schwettmann, and D. Blume, “Mean-field spin-oscillation dynamics beyond the single-mode approximation for a harmonically trapped spin-1 Bose-Einstein condensate,” *arXiv*, pp. 25–27, 2020.
- [19] C. Kam and R. B. Liu, “Berry phases of higher spins due to internal geometry of Majorana constellation and relation to quantum entanglement,” 2020.

# Chapter 5

## Conclusion

*”Student: Dr. Einstein, Aren’t these the same questions as last year’s [physics] final exam? Dr. Einstein: Yes; but this year the answers are different.”*

---

Albert Einstein

In this paper, we have used Majorana’s stellar representation to relate the Berry phase of spin-1 states to the Berry phase of its representative spin-1/2 states. We interpreted mean field spinor Bose-Einstein condensate dynamics under the single-mode approximation using the MSR, demonstrating that the spin-1 case leads to precession about the barycenter of the two normals and touching on aspects of the spin-2 dynamics. Using this, we derived expressions for the Berry phase in this regime and also outlined a method to estimate s-wave scattering constants.

The geometric intuition provided by the stellar representation is useful, but the method comes with the disadvantage of losing information about the phase of the state. In the mean field equations of motion, this results in one of interaction terms not contributing to the dynamics in the stellar representation. Consequently, only one of the scattering constants may be obtained by examining the time period of the spin-1 system.

The spinor BEC calculations were done under the SMA, ignoring Zeeman effects. The SMA is frequently employed to study these systems [1, 2] and simplifies the dynamics in the MSR, but for a more complete understanding, this assumption can be dropped. Analytical work in

this case for spin-1 and spin-2 systems [3, 4] can be compared to the dynamics of the MSR.

We also enforced zero linear and quadratic Zeeman terms and zero potential. In the spin-1 case, dropping these assumptions will result in deviation from the circular trajectories; this can be investigated in future works. Some work has been done on spin-1 systems in interesting traps [5, 6] - these results can be compared to the dynamics of the MSR.

Finally, we have looked solely at the addition of two bosons to form spin-1 and spin-2 systems, but fermions can also undergo condensation by forming molecules or via Cooper pairs. It is known that the behaviour of fermionic condensates is substantially different from BECs [7] - it would be interesting to see how Majorana dynamics differ.

More broadly, the role of geometry in quantum mechanics can be investigated further at a higher level. Hydrodynamics of BECs provide a natural area for investigating developments in geometric mechanics such as [8].

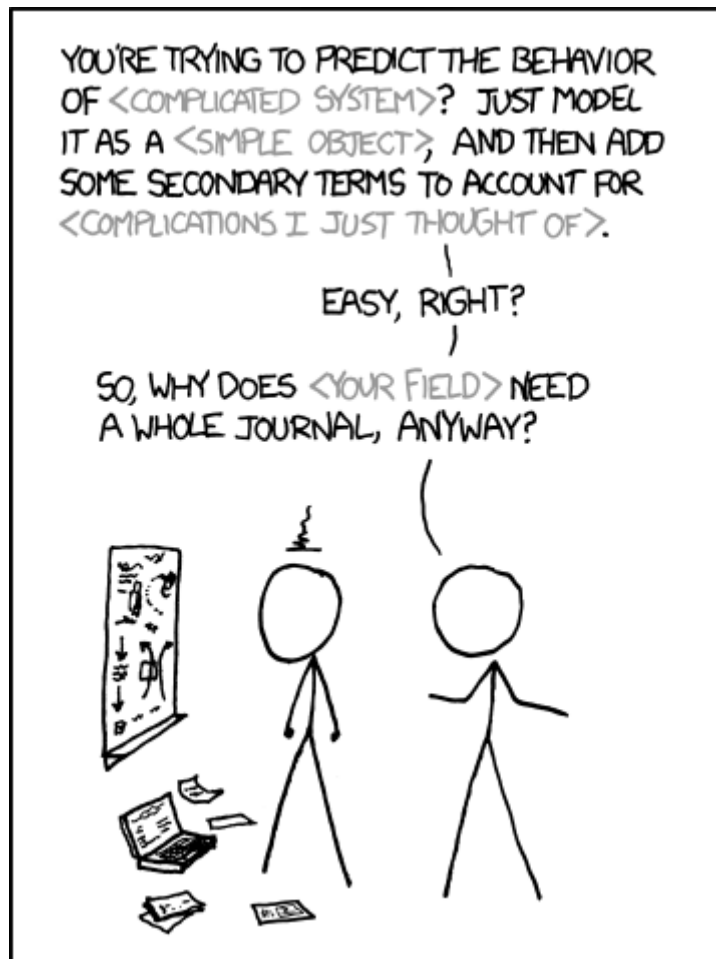


Figure 5.1: xkcd 793

## References

- [1] T.-L. Ho and S. K. Yip, “Fragmented and Single Condensate Ground States of Spin-1 Bose Gas,” *Physical Review Letters*, vol. 84, pp. 4031–4034, May 2000.
- [2] M. Koashi and M. Ueda, “Exact Eigenstates and Magnetic Response of Spin-1 and Spin-2 Bose-Einstein Condensates,” *Physical Review Letters*, vol. 84, pp. 1066–1069, Feb. 2000.
- [3] M. Ueda, *Fundamentals and new frontiers of Bose-Einstein condensation*. World Scientific Publishing Co., Jan. 2010.
- [4] Y. Kawaguchia and M. Uedaa, “Spinor Bose-Einstein condensates,” *Physics Reports*, vol. 520, no. 5, pp. 253–381, 2012.
- [5] P. Peng, G. Q. Li, W. L. Yang, and Z. Y. Yang, “Ground-states and rotational properties of a spin-orbit-coupled spin-1 Bose-Einstein condensate in a concentrically coupled toroidal trap,” *Physics Letters, Section A: General, Atomic and Solid State Physics*, vol. 382, no. 36, 2018.
- [6] A. M. Kamchatnov and V. S. Shchesnovich, “Dynamics of Bose-Einstein condensates in cigar-shaped traps,” *Physical Review A*, vol. 70, p. 23604, Aug. 2004.
- [7] M. Greiner, C. A. Regal, and D. S. Jin, “Emergence of a molecular Bose-Einstein condensate from a Fermi gas,” *Nature*, vol. 426, no. 6966, pp. 537–540, 2003.
- [8] M. S. Foskett, D. D. Holm, and C. Tronci, “Geometry of Nonadiabatic Quantum Hydrodynamics,” *Acta Applicandae Mathematicae*, vol. 162, no. 1, pp. 63–103, 2019.

# Appendix A

## Numerics

All plots and numerical calculations in this report were performed using the Quantum Toolbox in Python (QuTiP) [1, 2]. Python tests were performed (using pytest) to verify that the analytical results from Chapter 4 hold for spin-1, in particular, that  $\vec{m}$ ,  $\vec{n}_1 + \vec{n}_2$  and  $\vec{n}_1 \cdot \vec{n}_2$  are conserved.

## References

- [1] J. R. Johansson, P. D. Nation, and F. Nori, “QuTiP: An open-source Python framework for the dynamics of open quantum systems,” *Computer Physics Communications*, vol. 183, pp. 1760–1772, Aug. 2012.
- [2] J. R. Johansson, P. D. Nation, and F. Nori, “QuTiP 2: A Python framework for the dynamics of open quantum systems,” *Computer Physics Communications*, vol. 184, pp. 1234–1240, Apr. 2013.